THE JOURNAL OF BIOLOGICAL CHEMISTRY
Vol. 279, No. 48, Issue of November 26, pp. 50230–50242, 2004

Printed in U.S.A.

Identification of All-*trans*-Retinol:All-*trans*-13,14-dihydroretinol Saturase*

Received for publication, August 10, 2004, and in revised form, September 7, 2004
Published, JBC Papers in Press, September 9, 2004, DOI 10.1074/jbc.M409130200

Alexander R. Moise‡§, Vladimir Kuksa‡, Yoshikazu Imanishi‡, and Krzysztof Palczewski‡¶‖**

From the Departments of ‡Ophthalmology, ¶Pharmacology, and ‖Chemistry, University of Washington, Seattle, Washington 98195

Retinoids carry out essential functions in vertebrate development and vision. Many of the retinoid processing enzymes remain to be identified at the molecular level. To expand the knowledge of retinoid biochemistry in vertebrates, we studied the enzymes involved in plant metabolism of carotenoids, a related group of compounds. We identified a family of vertebrate enzymes that share significant similarity and a putative phytoene desaturase domain with a recently described plant carotenoid isomerase (CRTISO), which isomerizes prolycopene to all-*trans*-lycopene. Comparison of heterologously expressed mouse and plant enzymes indicates that unlike plant CRTISO, the CRTISO-related mouse enzyme is inactive toward prolycopene. Instead, the CRTISO-related mouse enzyme is a retinol saturase carrying out the saturation of the 13–14 double bond of all-*trans*-retinol to produce all-*trans*-13,14-dihydroretinol. The product of mouse retinol saturase (RetSat) has a shifted UV absorbance maximum, λ_{max} = 290 nm, compared with the parent compound, all-*trans*-retinol (λ_{max} = 325 nm), and its MS analysis (*m/z* = 288) indicates saturation of a double bond. The product was further identified as all-*trans*-13,14-dihydroretinol, since its characteristics were identical to those of a synthetic standard. Mouse RetSat is membrane-associated and expressed in many tissues, with the highest levels in liver, kidney, and intestine. All-*trans*-13,14-dihydroretinol was also detected in several tissues of animals maintained on a normal diet. Thus, saturation of all-*trans*-retinol to all-*trans*-13,14-dihydroretinol by RetSat produces a new metabolite of yet unknown biological function.

Retinoids are essential for many important biological functions, such as development, immunity, cellular differentiation, and vision of vertebrates. Retinoids encompassing both natural derivatives of all-*trans*-retinol and their synthetic analogues exert their functions through several active compounds. Esterification of retinol by lecithin-retinol acyltransferase (LRAT)[1] leads to retinyl esters, which represent both a major storage form of vitamin A and an intermediate of the visual cycle (1–3). In retinal pigment epithelium (RPE), an unidentified enzyme carries out the isomerization of all-*trans*-retinol either directly or through an ester intermediate to generate 11-*cis*-retinol, which can be oxidized to 11-*cis*-retinal, the visual chromophore (4). Reversible oxidation to retinal can be carried out by several members of the microsomal, short-chain alcohol dehydrogenase family and possibly by class I, III, and IV medium-chain alcohol dehydrogenases (5, 6). Oxidation of retinal by retinal dehydrogenase types 1, 2, 3, and 4 generates retinoic acid (RA) (7–12), which controls development and cellular differentiation via nuclear receptors (13). RA-inducible cytochrome P450 enzymes CYP26A1, B1, and C1 carry out the catabolism of RA to polar 4-hydroxy-RA, 4-oxo-RA, and 18-hydroxy-RA (14–17). Specific localization of RA anabolizing and catabolizing enzymes are essential for embryonic patterning. Other pathways generate *retro*-retinoids such as 14-hydroxy-4,14-retro-retinol (18) and anhydroretinol (19), whose opposing effects control cell growth. Given the low levels and labile nature of retinoids in biological systems and the incompletely understood mechanism of their biotransformations, many of the enzymes involved in retinoid metabolism remain to be discovered.

In addition to dietary sources, retinoids are derived from the cleavage of C_{40} provitamin A carotenoids such as α- and β-carotene and cryptoxanthin to produce retinal, which can be converted to all-*trans*-retinol. Provitamin A carotenoids also represent a major storage form of retinoids in tissues, serum, and the vertebrate egg yolk. Only two enzymes involved in the metabolism of β-carotene in animals have been identified: β,β-carotene-15,15′-monooxygenase (BCO-I) (20), which carries out the symmetric cleavage of β-carotene to produce retinal, and β,β-carotene-9′,10′-oxygenase (BCO-II), which carries out the asymmetric cleavage to generate β-ionone and β-apo-10′-carotenal (21). BCO-I and -II have sequence similarity to VP14, the 9-*cis*-neoxanthin cleavage enzyme from *Zea mais*, and other carotenoid cleavage enzymes from plants (reviewed in Ref. 22). BCO-I was first identified in flies based on its similarity to VP14 (20) and later cloned from mice (23) and humans (24). Other, more limited dietary sources of retinoids are all-*trans*-retinyl esters and free all-*trans*-retinol. In addition to β-carotene, retinal, and retinoic acid, animal tissues also retain considerable amounts of nonprovitamin A carotenoids such as

* The costs of publication of this article were defrayed in part by the payment of page charges. This article must therefore be hereby marked "*advertisement*" in accordance with 18 U.S.C. Section 1734 solely to indicate this fact.

The nucleotide sequence(s) reported in this paper has been submitted to the GenBank™/EBI Data Bank with accession number(s) AY704159 (for mouse RetSat), AY707524 (for monkey (macaque) RetSat).

§ To whom correspondence may be addressed: Dept. of Ophthalmology, University of Washington, Box 356485, Seattle, WA 98195-6485. Tel.: 206-543-9074; Fax: 206-221-6784; E-mail: moise@u.washington.edu.

** To whom correspondence may be addressed: Dept. of Ophthalmology, University of Washington, Box 356485, Seattle, WA 98195-6485. Tel.: 206-543-9074; Fax: 206-221-6784; E-mail: palczews@u.washington.edu.

[1] The abbreviations used are: LRAT, lecithin-retinol acyltransferase; BCO-I, β,β-carotene-15,15′-monooxygenase; BCO-II, β,β-carotene-9′,10′-oxygenase; CRTISO, carotenoid isomerase(s); MS, mass spectrometry; ER, endoplasmic reticulum; HPLC, high performance liquid chromatography; RA, retinoic acid; RetSat, all-*trans*-(13,14)-retinol saturase; RPE, retinal pigment epithelium; Tet, tetracycline; PBS, phosphate-buffered saline.

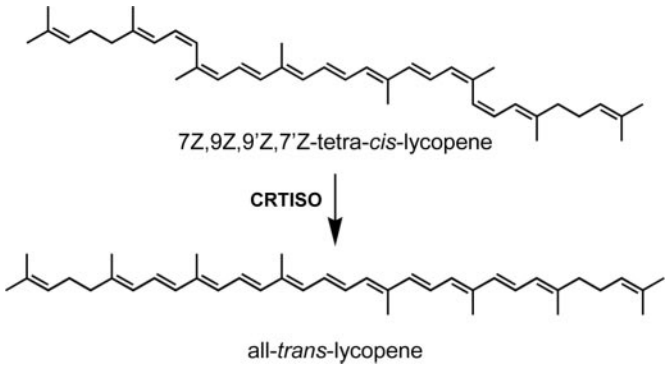

SCHEME 1. **Reaction catalyzed by plant and cyanobacterial CRTISO.**

lutein and zeaxanthin in the primate macula and lycopene in serum and most tissues. Nonprovitamin A carotenoids as well as uncleaved β-carotene have been implicated in the prevention of cancer, macular degeneration, and heart disease (reviewed in Refs. 25 and 26). Despite this interest, the enzymes involved in the metabolism and physiology of carotenoids in animals await molecular identification.

Powerful genetic approaches and readily identifiable phenotypes aided in the discovery of the biochemical pathways of carotenoid synthesis in plants and bacteria. These enzymes could serve as a model to uncover carotenoid or retinoid enzymes in vertebrates. Recently, the enzymes responsible for the isomerization of (7*Z*,9*Z*,9′*Z*,7′*Z*)-tetra-*cis*-lycopene (also known as prolycopene) to all-*trans*-lycopene in plants (27, 28) and cyanobacterium *Synechocystis* (29, 30) (Scheme 1) have been characterized (reviewed in Ref. 31). Tomato CRTISO mutants are known for their *tangerine* phenotype due to accumulation of (7*Z*,9*Z*,9′*Z*,7′*Z*)-tetra-*cis*-lycopene (32). The protein sequences of CRTISO enzymes are similar to CrtI from nonphotosynthetic bacteria, an enzyme that catalyzes the direct conversion of phytoene into all-*trans*-lycopene (33). It also bears resemblance to phytoene desaturase and ζ-carotene desaturase from plants, which each introduce two double bonds during the four desaturation steps from phytoene to (7*Z*,9*Z*,9′*Z*,7′*Z*)-tetra-*cis*-lycopene (*trans*-H elimination at 11,11′ by phytoene desaturase and *cis*-H elimination at 7,7′ by ζ-carotene desaturase) (reviewed in Ref. 34).

Searching for homologous proteins using the protein sequences of plant CRTISO, we found similarities in a few hypothetical proteins predicted by the conceptual translation of expressed sequence tags and transcripts from vertebrates and nonvertebrates. Expression of the mouse CRTISO-like protein in transfected cells revealed that it catalyzes saturation of all-*trans*-retinol at the 13–14 double bond, and the mouse CRTISO-like protein was thus designated RetSat. This is in contrast to tomato CRTISO, which catalyzes *cis-trans* isomerization of lycopene and has no saturase activity *versus* all-*trans*-retinol. Moreover, the saturated product, all-*trans*-13,14-dihydroretinol, is detected in several tissues of animals maintained on a diet containing normal levels of vitamin A.

MATERIALS AND METHODS

Cloning of Mouse and Monkey RetSat and Tomato CRTISO and Creation of Stable Cell Lines with Inducible Expression—RPE was microdissected from a C57/BL6 mouse or macaque crab-eating monkey (*Macaca fascicularis*). RNA from mouse or monkey RPE and from ripe, red tomato was isolated using the MicroAqueous RNA Isolation Kit (Ambion, Austin, TX) and reverse-transcribed using SuperScript II reverse transcriptase (Invitrogen) and oligo(dT) primers according to the manufacturer's protocol. Mouse RetSat cDNA was amplified using Hotstart Turbo *Pfu* Polymerase (Stratagene, La Jolla, CA) and the primers 5′-ATGTGGATCACTGCTCTGCTGCTGG-3′ (forward) and 5′-TCTGGCTCTTCTCTGAACGGACTACATC-3′ (reverse); monkey RetSat was amplified with primers 5′-CAGTCGGAGCTGTCCCATTTACC-3′ (forward) and 5′-AAATTCCTCTGACTCCTCCCTGATG-3′ (reverse); tomato CRTISO was amplified using the primers 5′-CTTTCCAGGGAGCCCAAAAT-3′ (forward) and 5′-ACATCTAGATATCATGCTAGTGTCCTT-3′ (reverse). For expression of mouse RetSat, cDNA was amplified with the primers 5′-CCTCTAGAGCCACCATGTGGATCACTGCTCTGCTGCTGG-3′ (forward) and 5′-ACTAGTCTACATCTTCTTCTTTTGTGCCTTGACCTTTGA-3′ (reverse) and cloned into the tetracycline-inducible, eukaryotic expression vector pcDNA4/TO (Invitrogen) using XbaI/SpeI, whereas tomato CRTISO was amplified using the primers 5′-TCTAGAAGGAGGACAGCAATGGTAGATGTAGACAAAAGAGTGGA-3′ (forward) and 5′-ACATCTAGATATCATGCTAGTGTCCTT-3′ (reverse) and cloned into the XbaI site of pcDNA4/TO. *N*-Acetylglucosaminyltransferase I-negative HEK293S cells, obtained from Dr. G. Khorana (MIT, Boston, MA), were transfected with the *tetR* expression plasmid pcDNA6-TR(blaR), and blasticidin-resistant colonies were selected and cloned. A stable *tetR*-expressing clone of HEK-293S designated HEK-Khorana (HEKK) was then transfected with pcDNA4/TO (zeoR) containing either mouse RetSat or tomato CRTISO cDNA and selected with zeocin. All zeocin-resistant clones were pooled and used in activity assays. Cells were cultured in Dulbecco's modified Eagle's medium, 10% fetal calf serum plus zeocin and blasticidin antibiotics and maintained at 37 °C, 5% CO_2, and 100% humidity.

Inducible Expression of LRAT Protein in HEKK Cells—Mouse LRAT cDNA was cloned as described elsewhere (2). For expression, LRAT coding region was amplified using the primers 5′-GCCACCATGAAGAACCCAATGCTGGAAGCT-3′ and ACATACACGTTGACCTGTGGACTG. The PCR product was ligated into the pCR-Blunt II-TOPO vector (Invitrogen) and then subcloned into the EcoRI site of pcDNA4/TO. *TetR*-expressing HEKK cells were transfected with the pcDNA4/TO-LRAT construct and selected with zeocin. Stable clones were verified for expression of LRAT protein using the anti-LRAT monoclonal antibody described elsewhere (2).

Purification of a Bacterially Expressed His-tagged Mouse RetSat Fragment, Polyclonal and Monoclonal Antibody Production—The NcoI fragment of RetSat cDNA, corresponding to nucleotides 440–1391 of mouse RetSat cDNA (coding for the ^{148}MASPF . . . MTALVPM^{465} polypeptide fragment) was cloned into the NcoI site of the inducible bacterial expression vector pET30B (Invitrogen). This resulted in a recombinant protein tagged at both amino and carboxyl termini with hexahistidine tags. The plasmid was transformed into BL-21RP cells (Stratagene), and expression was induced with isopropyl-1-thio-β-D-galactopyranoside. The double His_6-tagged fragment of the mouse RetSat protein (40 kDa) was purified by Ni^{2+}-nitrilotriacetic acid affinity using the manufacturer's protocol (Qiagen, Valencia, CA). The purified protein was examined by gel electrophoresis. Following in-gel trypsin digestion, the eluted tryptic peptides were examined by microsequencing by liquid chromatography/mass spectrometry to verify the identity of the recombinant RetSat fragment (not shown). The purified protein was used to immunize mice as described before (35), and the monoclonal antibody was produced by established methods (36). Rabbit polyclonal antiserum was raised in collaboration with Cocalico Biologicals Inc. (Reamstown, PA). The sera and monoclonal antibody were tested for their specificity by immunocytochemistry and immunoblotting of RetSat-transfected *versus* untransfected cells. Anti-RetSat IgG was purified from the ascitic supernatant of RetSat-producing hybridoma cells using a HiTRAP protein G HP (Amersham Biosciences), using the manufacturer's protocol. The purified antibody was coupled with fluorophore using the Alexa Fluor 488 monoclonal antibody coupling kit (Invitrogen) following the manufacturer's protocol.

Northern Blot Analysis of Mouse RetSat Transcripts—Northern blot analysis was performed using a commercially available premade blot containing 2 μg of poly(A) RNA from various mouse tissues per lane (FirstChoice Northern blot Mouse Blot I; Ambion) following the manufacturer's protocol. The α-^{32}P-radiolabeled probe was constructed by run-off PCR of mouse RetSat cDNA using the 5′-TCTGGCTCTTCTCTGAACGGACTACATC-3′ reverse primer and the Strip-EZ probe synthesis kit from Ambion following the manufacturer's protocol. Alternatively, a radiolabeled antisense mouse beta-actin probe was constructed using the T7 primer and the pTRIamp18 β-actin template (Ambion).

Immunoblotting and Immunohistochemistry Analysis of Mouse RetSat—To establish the membrane association of RetSat, mouse liver was homogenized in 50 mM Tris-HCl, pH 8.0, containing 250 mM sucrose, 5 mM dithiothreitol, and 1× protease inhibitor mixture (Sigma) using a Dounce homogenizer. The nuclei and extracellular matrix were pelleted by centrifugation for 30 min at 20,000 × *g* and discarded. The high

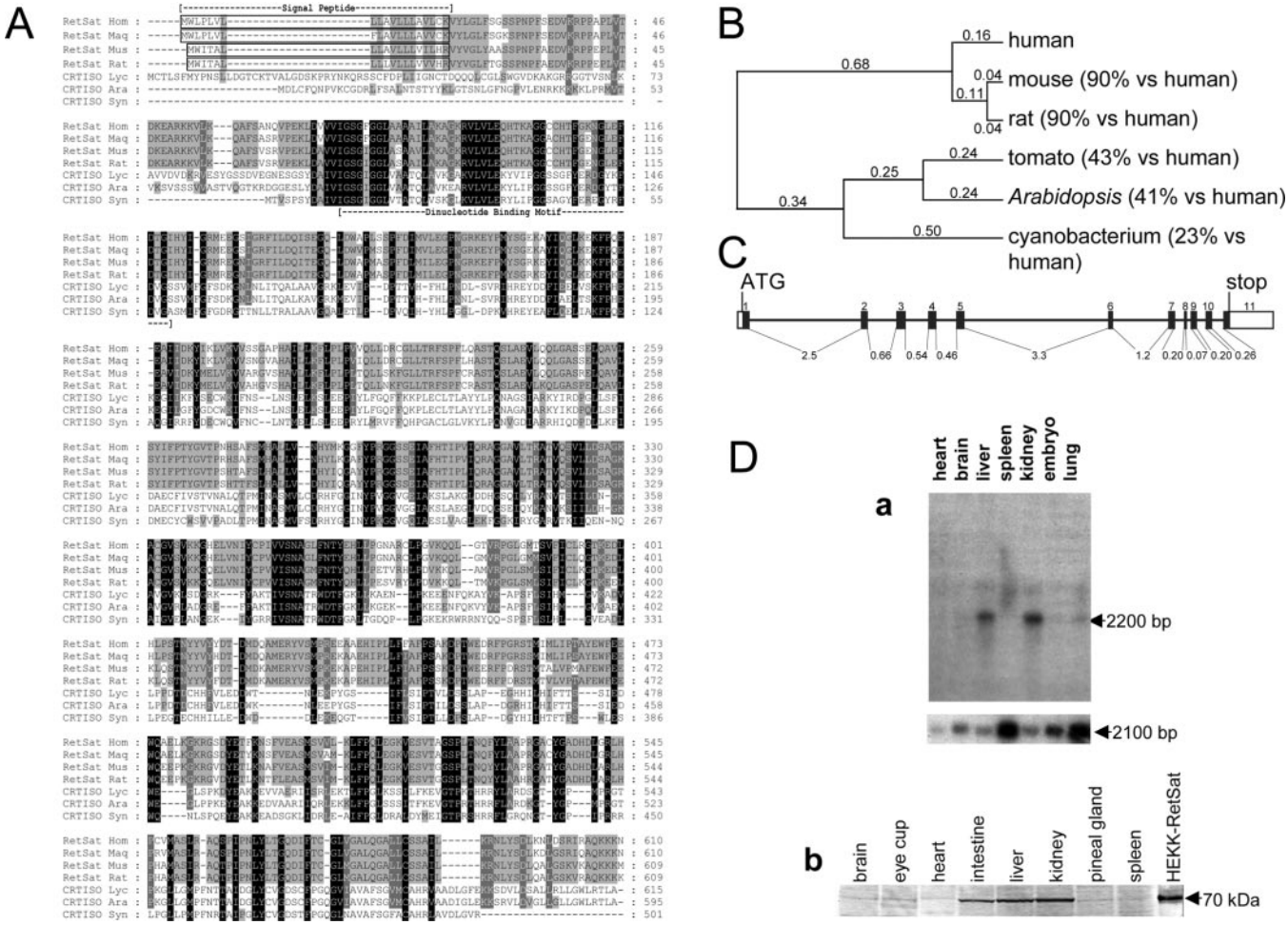

FIG. 1. **Identification of vertebrate proteins with similarity to plant and cyanobacteria CRTISO.** *A*, sequence comparison of human RetSat (RetSat Hom-gi46329587), macaque-monkey RetSat (RetSat Maq-AY707524 submitted sequence), mouse RetSat (RetSat Mus-AY704159 submitted sequence), and rat RetSat (RetSat Rat-gi34855900) with tomato CRTISO (CRTISO Lyc-gi19550437), *Arabidopsis* CRTISO (CRTISO Ara-gi42561764), and cyanobacterial CRTISO (CRTISO Syn-gi16331999). *White letters* on a *black background* represent identical residues. *White letters* on a *gray background* represent conserved substitutions in all but one of the species examined, whereas *black letters* on a *light gray background* indicate substitutions conserved in four of the seven species examined. The *dashed lines* represent gaps introduced to maximize the alignment. The alignment was built using the program T-Coffee and the matrix BLOSUM62 (64) with gap penalties: existence-11, extension-1. Sequence-based predictions such as the signal peptide and a putative dinucleotide binding motif are indicated. A phylogenetic tree of CRTISO-like enzymes was built using the ClustalW neighbor-joining distance algorithm with *numbers* indicating evolutionary distances (65) (*B*). The percentage similarity to human RetSat is indicated in *parentheses beside* the gene name. *C*, gene structure of human RetSat as it is found on the minus strand of chromosome 2 from 85,556,195 to 85,543,754. The *numbered black boxes* indicate exons, *white boxes* indicate untranslated regions, and *lines* represent introns. The length of each intron is indicated in kbp. The start (ATG) and stop of translation are also indicated. *D*, tissue distribution of mouse RetSat. *a*, Northern blot analysis of mouse RetSat expression in various mouse tissues (*top panel*) indicates that mouse RetSat is expressed predominantly in the liver and kidney among the tissues examined. Control hybridization was performed by stripping and reprobing of the same blot using an antisense probe to nonmuscle β-actin (*bottom panel*). The size of detected transcripts is shown at the *right side* of the *panels*. Lysates of various mouse tissues containing 10 μg of protein per lane were subjected to immunoblotting using rabbit polyclonal anti-mouse RetSat serum (*b*). The *lane labeled HEKK-RetSat* shows the immunoreactivity of the mouse RetSat protein from the lysate of Tet-induced, HEKK-RetSat cells corresponding to 1 μg of total loaded protein. There is no immunoreactive band in the lysate of untransfected cells immunoblotted with either rabbit polyclonal or mouse monoclonal antibody (not shown). The apparent molecular mass of mouse RetSat is 70 kDa and is indicated to the *right* of the *panel*.

speed cytosolic supernatant and postnuclear membranes were separated by centrifugation at 145,000 $\times$ *g* for 90 min. Postnuclear membranes were homogenized in 10 mM Tris, pH 8.0, containing 200 mM NaCl, 1 mM EDTA, 1% Triton X-100, and 10 μM phenylmethylsulfonyl fluoride. The protein concentration was measured in whole cell lysate, high speed cytosolic supernatant, and postnuclear membrane fraction using the Bradford assay (37). Equal amounts of protein were resolved on SDS-PAGE, transferred onto polyvinylidene difluoride membrane, and stained with a 1:1000 dilution of anti-RetSat monoclonal antibody and 1:10^4 goat anti-mouse IgG (Fc) (Promega, Madison, WI). To examine tissue-specific expression of RetSat, various mouse tissues were dissected and homogenized with 10 mM Tris, pH 8.0, containing 10 mM 2-mercaptoethanol and 10 μM phenylmethylsulfonyl fluoride, with the aid of a Dounce homogenizer. The membranes were pelleted by centrifugation at 12,000 $\times$ *g* for 30 min. The protein concentration was measured using the Bradford assay (37). Equal amounts of protein (10 μg) from the membrane fraction of each tissue were resolved by SDS-PAGE, transferred onto polyvinylidene difluoride membrane, and stained by immunoblotting with a 1:1000 dilution of rabbit anti-RetSat polyclonal antiserum and alkaline phosphatase-coupled 1/10^4 goat anti-rabbit IgG (Fc) (Promega) secondary antibody. The mouse monoclonal anti-RetSat showed the same reactivity in the examined tissues as the polyclonal antiserum. Untransfected HEKK or HEKK-RetSat cells were cultured in Dulbecco's modified Eagle's medium (Invitrogen) on glass bottom microwell dishes (MatTek Corp., Ashland, MA). Expression of RetSat was induced by the addition of 1 μg/ml tetracycline. Cells were harvested after 48 h and fixed with 4% paraformaldehyde (Fisher, Hampton, NH) in PBS (136 mM NaCl, 11.4 mM sodium phosphate, pH 7.4) for 10 min and washed by PBS. To block nonspecific labeling, the cells were incubated in 1.5% normal goat serum (Vector Laboratories, Inc., Burlingame, CA) in PBST (136 mM NaCl, 11.4 mM sodium phosphate, 0.1% Triton X-100, pH 7.4) for 15 min at room temperature. The cells were incubated overnight at 4 °C in Alexa 488-coupled anti-RetSat monoclonal IgG diluted with PBST. The sections were rinsed in PBST

and mounted in 50 μl of 2% 1,4-diazabicyclo-[2.2.2]octane (Sigma) in 90% glycerol to retard photobleaching. For confocal imaging, the cells were analyzed on a Zeiss LSM510 laser-scanning microscope.

Retinol Isomer Purification and HPLC Analysis of Retinoids—All procedures involving retinoids were performed under dim red light unless otherwise specified. Retinoids were stored in *N,N*-dimethylformamide under argon at −80°C. All retinol and retinal substrates were purified by normal phase HPLC (Beckman Ultrasphere-Si, 5 μm, 4.6 × 250 mm) with 10% ethyl acetate, 90% hexane at a flow rate of 1.4 ml/min using an HP1100 high performance liquid chromatograph with a diode-array detector and HP Chemstation A 08.03 software. For all-*trans*-13,14-dihydroretinol, we used an extinction coefficient ϵ = 16,500 at 290 nm. The following extinction coefficients were used for retinoids (in M^{-1} cm^{-1}): all-*trans*-retinol, ϵ = 51,770 at 325 nm; 9-*cis*-retinol, ϵ = 42,300 at 323 nm; 11-*cis*-retinol, ϵ = 34,320 at 318 nm; 13-*cis*-retinol, ϵ = 48,305 at 328 nm; all-*trans*-retinal, ϵ = 48,000 at 368 nm in hexane (38); and all-*trans*-retinoic acid, ϵ = 45,300 at 350 nm in ethanol. Retinoic acid was dissolved in ethanol and examined by a reverse-phase HPLC System II (Zorbax ODS, 5 μm, 4.6 × 250 mm; Agilent, Foster City, CA) with an isocratic mobile phase of 70% acetonitrile, 29% water, 1% glacial acetic acid and flow rate of 1.4 ml/min.

(7Z,9Z,9′Z,7′Z)-Tetra-cis-lycopene Purification and Reverse-phase HPLC Analysis of Carotenoids—Carotenoid extraction and analysis were performed under dim red light. One g from the fruit of a tangerine tomato was freeze-thawed three times and extracted with 2 ml of PBS, 2 ml of ethanol, and 6 ml of hexane with the aid of a Dounce homogenizer. The organic phase was dried and resuspended in ethanol/tetrahydrofuran (9:1) and examined by reverse-phase HPLC System I (Prontosil, 200-3-C30, 3 μm, 4.6 × 250 mm; Bischoff Chromatography, Leonberg, Germany) with a mobile phase of 75% *tert*-butyl methyl ether, 25% methanol and a flow rate of 1 ml/min. More than 90% of the extract consisted of (7*Z*,9*Z*,9′*Z*,7′*Z*)-tetra-*cis*-lycopene, which was identified based on its published UV-visible absorption spectrum in hexane (37) with the following characteristics: shoulder at λ = 417 nm, ϵ = 90,000 M^{-1} cm^{-1}, λ_{max} = 437 nm, ϵ = 105,000 M^{-1} cm^{-1}, shoulder at λ = 461 nm, ϵ = 70,000 M^{-1} cm^{-1}.

Enzyme Assays of RetSat- and CRTISO-catalyzed Reactions—For enzyme assay, cells were seeded in 6-well plates, and expression of RetSat or CRTISO was induced with 1 μg/ml tetracycline 48 h prior to analysis. Substrate preparation and addition were conducted under dim red light. Retinoid substrates were purified by HPLC as described above and dissolved in *N,N*-dimethylformamide to a final concentration of 4 mM. Organic extract of tangerine tomatoes was dried under a stream of argon and resuspended in *N,N*-dimethylformamide. The substrates were diluted in 300 μl of complete medium (tetracycline, 1 μg/ml) to a 40 μM final concentration, overlaid on cells, and incubated overnight in the dark at 37 °C in 5% CO_2 and 100% humidity. Media and cells were collected by scraping and mixed with an equal volume of methanol. For retinol and dihydroretinol analysis, the methanol/water mixture was extracted with two volumes of hexane, and then the organic phase was dried, resuspended in hexane, and analyzed by normal phase HPLC. Retinal and dihydroretinal analysis was performed by treatment of the methanol/water mixture with 12.5 mM hydroxylamine followed by organic extraction and normal phase HPLC. For carotenoid analysis, the organic phase was dried and resuspended in ethanol/tetrahydrofuran (9:1) and examined by reverse-phase HPLC System I. For retinoic acid analysis, the 1:1 methanol/water mixture was acidified with 0.1 volumes of 12 N HCl and extracted with 1 volume of chloroform, dried, and resuspended in ethanol and examined by reverse-phase HPLC System II.

Chemical Synthesis of All-trans-13,14-dihydroretinol—All reagents were purchased from Sigma or Fluka and were used without additional purification. Solvents were dried under standard procedures prior to use. All operations with retinoids were performed under dim red light unless otherwise specified. β-Ionone was condensed with triethyl phosphonoacetate in anhydrous tetrahydrofuran in the presence of NaH to give ethyl *trans*-β-ionylideneacetate. This ester was then reduced with $LiAlH_4$ to alcohol and reacted overnight with triphenylphosphine hydrobromide to give Wittig salt. Ethyl 4-oxo-3-methylcrotonate was hydrogenated in methanol with H_2 using 10% palladium on carbon as a catalyst to yield ethyl 4-oxo-3-methylbutyrate, which was then reacted with Wittig salt using *t*-BuOK as a base in anhydrous CH_2Cl_2 in the presence of 18-crown-6. The obtained mixture of ethyl 11-*cis*- and all-*trans*-13,14-dihydroretinoates was reduced with $LiAlH_4$ to 13,14-dihydroretinols, and all-*trans*-isomer was separated from 11-*cis*-dihydroretinol by flash chromatography of silica gel using 5% ethyl acetate in hexane. NMR data were recorded on a Bruker 500-MHz spectrometer using $CDCl_3$ as an internal standard. ^1H NMR analysis of synthetic all-*trans*-13,14-dihydroretinol: NMR ($CDCl_3$, δ, ppm) 6.41 (dd, 1H, H-12, *J* = 11.3, 14.75 Hz), 6.10–6.12 (m, 3H, H-7, H-8, H-10, *J* = 15.7 Hz), 5.6 (dd, 1H, H-11, *J* = 8.34, 14.95 Hz), 3.67 (m, 2H, CH_2-15), 2.41 (m, 1H, H-13, *J* = 6.7 Hz), 1.96 (m, 2H, CH_2-14), 1.90 (s, 3H, CH_3-9), 1.69 (s, 3H, CH_3-5), 1.46 (m, 2H, CH_2-2), 1.6 (m, 4H, CH_2-3, CH_2-4), 1.06 (d, 3H, CH_3-13 *J* = 6.7 Hz), 1.00 (s, 6H, 2× CH_3-1).

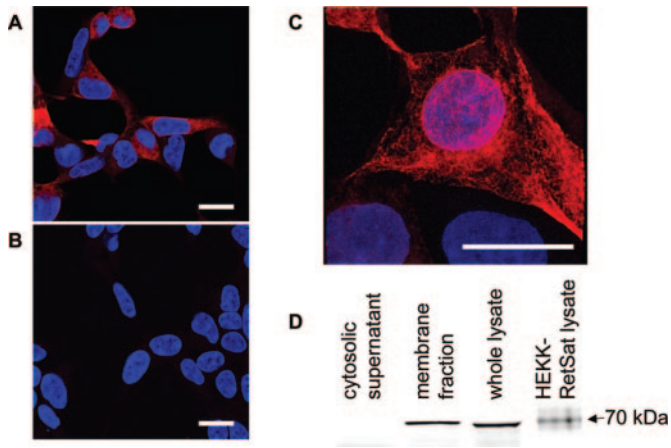

FIG. 2. **Subcellular localization of mouse RetSat in transfected cells.** The anti-mouse RetSat monoclonal antibody (*red*) was used to stain Tet-induced HEKK-RetSat-transfected cells (*A*) and untransfected cells (*B*). HEKK-RetSat cells stained with the anti-RetSat monoclonal antibody examined under higher magnification show the perinuclear and reticular membrane localization of RetSat in transfected cells (*C*). *Scale bar*, 20 μm. *D*, subcellular analysis of RetSat protein in mouse liver cells. Immunoblotting of equal amounts of protein from the cytosolic supernatant, postnuclear membrane fraction, and whole cell lysate of mouse liver cells indicates that the RetSat protein is membrane-associated. An immunoreactive band of a protein with apparent molecular mass of 70 kDa was identified as the mouse RetSat protein, confirmed by its presence in the lysate of Tet-induced HEKK-RetSat cells. The blots were probed with the anti-mouse RetSat monoclonal antibody.

Isomerization and Electron Impact Mass Spectrometry Analysis of All-trans-13,14-dihydroretinol—Equal amounts (by UV absorbance) of the synthetic and biosynthetic compounds were resuspended in ethanol and exposed to sunlight for 30 min, followed by the addition of an equal volume of water and two volumes of hexane. The compounds were extracted, the organic phase was dried and resuspended in hexane, and the isomeric mixture was examined by normal phase HPLC. For MS analysis, the unknown biosynthetic metabolite and the chemically synthesized all-*trans*-13,14-dihydroretinol were purified by normal phase HPLC and analyzed by electron impact mass spectrometry analysis using a JEOL HX-110 direct probe mass spectrometer. Some of the ions in the fragmentation patterns of both samples were as follows: 288 $[M]^+$, 273 $[M\text{-}CH_3]^+$, 243 $[M\text{-}CH_2CH_2OH]^+$, 215 $[M\text{-}CH(Me)(CH_2)_2OH]^+$, 202, 187, 159. The spectra are shown without manipulation.

Enzymatic Assays for Saturase Activity in Homogenized Cells—Cells were homogenized with 15 mM Tris-HCl, pH 8.0, containing 10 mM dithiothreitol and 0.32 M sucrose. One aliquot of cells was boiled for 10 min at 95 °C as a negative control. Cell aliquots of 200 μl were supplemented with 1 mM ATP and 40 μM all-*trans*-retinol final concentrations. Some aliquots were also supplemented with 0.4 mM NADH or 0.4 mM NADPH to regenerate the redox state of the reaction. The cell homogenate was incubated with retinol substrate with shaking at 37 °C for 1 h in the dark. This was followed by the extraction of retinoids with one volume of methanol and two volumes of hexane. The organic phase was dried and resuspended in hexane and then examined by normal phase HPLC.

Esterification Assay of All-trans-retinol and All-trans-13,14-dihydroretinol—HEKK-LRAT cells were homogenized in 250 mM sucrose, 10 mM Tris-HCl with the aid of a Dounce homogenizer. RPE microsomes were prepared as previously described (39). A substrate solution, 2 μl of 1 mM stock in *N,N*-dimethylformamide, was added to a 1.5-ml Eppendorf tube containing 20 μl of 10% bovine serum albumin and 20 μl of UV-treated RPE microsomes or 100 μl of membrane homogenate of HEKK-LRAT cells and 10 mM BTP (pH 7.5) buffer to a total volume of 200 μl. The reactions were incubated at 37 °C for 10 min. Retinoids were extracted with 300 μl of methanol and 300 μl of

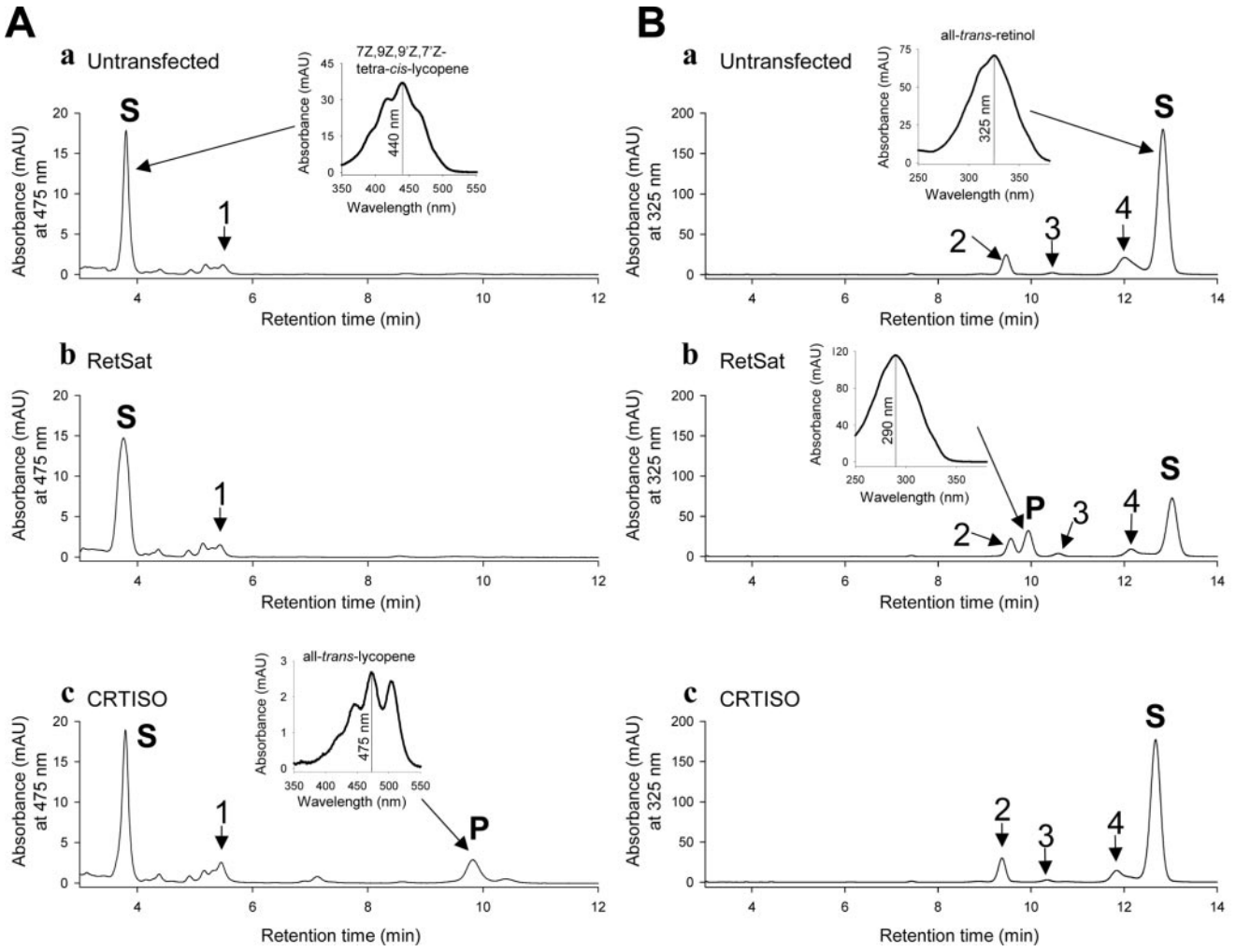

FIG. 3. **Enzyme activities of tomato CRTISO and mouse RetSat in transfected cells.** *A*, analysis of the effect of tomato CRTISO and mouse RetSat on the conversion of (7*Z*,9*Z*,9′*Z*,7′*Z*)-tetra-*cis*-lycopene into all-*trans*-lycopene. Cells were incubated with (7*Z*,9*Z*,9′*Z*,7′*Z*)-tetra-*cis*-lycopene substrate (*S*), extracted, and examined by reverse-phase HPLC System I for the conversion of *S* into all-*trans*-lycopene product (*P*). The analysis indicates that the conversion occurs in cells expressing tomato CRTISO (*c*) but not in untransfected (*a*) or RetSat-expressing cells (*b*). A compound whose absorbance spectrum corresponds to 7,9-di-*cis*-lycopene was observed in all cells and more intensely in CRTISO-expressing cells (indicated by *1*). *B*, analysis of the effect of tomato CRTISO and mouse RetSat on the conversion of all-*trans*-retinol into a new product. Cells were incubated with all-*trans*-retinol substrate (*S*), extracted, and examined by normal phase HPLC for the conversion of *S* into a novel product (*P*) whose maximum absorbance peak is 290 nm. The analysis indicates that the conversion occurs in cells expressing mouse RetSat (*b*) but not in untransfected (*a*) or CRTISO-expressing cells (*c*). Additional peaks with absorbance spectra corresponding to 13-*cis*-retinol (*2*), 9,13-di-*cis*-retinol (*3*), and 9-*cis*-retinol (*4*) were observed in all cells regardless of background and are most likely the result of thermal isomerization. The experiment was performed in duplicate samples and repeated. *mAU*, milliabsorbance units.

hexane. Then 100 μl of the hexane extract was analyzed by normal phase HPLC, using first 0.5% ethyl acetate in hexane for 10 min to separate retinyl esters and then 20% ethyl acetate in hexane for an additional 10 min to separate retinols. Elution was monitored at 290 and 325 nm.

RESULTS

Cloning of the cDNA of Mouse and Monkey CRTISO-like Proteins—The protein sequences of tomato and *A. thaliana* CRTISO were used to search for similar proteins in other species. We found proteins that share extensive similarity over the entire length of the protein in several phyla, from bacterial, archaebacterial, and fungal phytoene desaturases to other desaturase and CRTISO-like proteins in other plants and higher eukaryotes. A family of highly conserved proteins was found in many chordate species but not in nonchordates. This chordate CRTISO-like protein family has members in vertebrates such as humans, mice, rats, chickens, and zebrafish and pufferfish (*Fugu rubipres* and *Tetraodon nigroviridis*) as well as invertebrates such as the ascidians *Ciona intestinalis* and *Ciona savignyi*. The CRTISO-like ascidian proteins share many conserved residues with the related vertebrate proteins as judged by the translation of the available ascidian genomic sequence (63% conserved substitutions including 41% identical residues compared with humans). The alignment of the human, monkey, mouse, and rat protein sequences to CRTISO from tomato, *A. thaliana*, and cyanobacterium *Synechocystis* sp. (strain PCC 6803) is represented in Fig. 1*A*. Vertebrate CRTISO-like proteins are named RetSat after the catalytic activity observed for this enzyme (see below). A phylogenetic dendogram based on a neighbor-joining algorithm appears to be monophyletic (Fig. 1*B*) and indicates that the proteins found in vertebrates are related to plant CRTISO (41–43% conserved substitutions including 25–27% identical residues). Thus, the ancestral member of plant CRTISO and vertebrate RetSat appeared before the divergence of plant and animal kingdoms. Not only do mouse, human, and rat RetSat proteins share extensive homology throughout their sequence, but the genes coding for these proteins have the same exon-intron arrangement, with the intron breaks at the same place in the aligned protein sequence. The human gene encompasses 12 kbp of genomic DNA

SCHEME 2. **Synthesis of all-*trans*-13,14-dihydroretinol.** *a*, $(EtO)_2P(O)$-CH_2COOEt. NaH, tetrahydrofuran, room temperature, 24 h; *b*, $LiAlH_4$, Et_2O, 0 °C, 30 min; *c*, Ph_3P·HBr, MeOH, room temperature, 24 h; *d*, H_2 (bar), MeOH, Pd/C, room temperature, 24 h; *e*, *tert*-BuOK, 18-crown-6, CH_2Cl_2, room temperature to −78 °C to room temperature, 12 h.

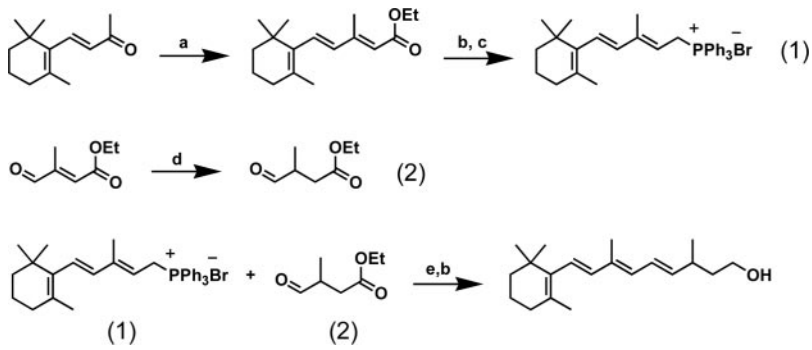

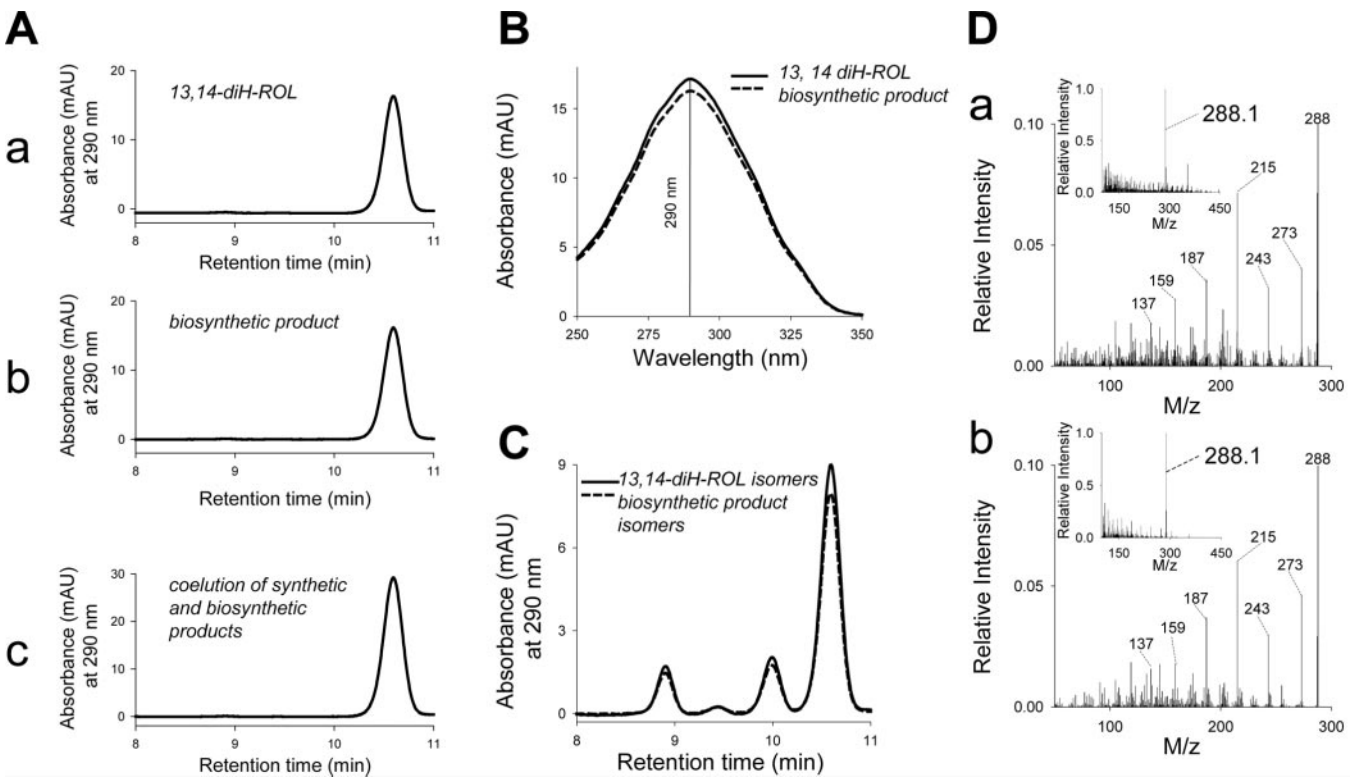

FIG. 4. **Identification of the biosynthetic product of the conversion of all-*trans*-retinol by mouse RetSat.** The HPLC-purified biosynthetic product of the RetSat reaction was compared with 13,14-dihydroretinol for its elution characteristics on normal phase HPLC (*A*). The retention times for both all-*trans*-13,14-dihydroretinol (*a*) and the biosynthetic product (*b*) are identical, and when mixed, the two compounds co-elute as a single peak (*c*). The absorbance spectrum for the two compounds is identical with a maximum absorbance at 290 nm (*B*). Both all-*trans*-13,14-dihydroretinol and the biosynthetic compound generate the same pattern of isomers following light-induced isomerization (*C*). Electron impact MS analysis of the biosynthetic product (*a*) and all-*trans*-13,14-dihydroretinol (*b*) shows that they have the same mass of 288 *m/z*, corresponding to retinol plus 2H (*D*). The base peak is shown in the *inset*. The MS fragmentation patterns of biosynthetic compound (*a*) and all-*trans*-13,14-dihydroretinol compound (*b*) show that they generate ions of the same mass and relative intensity. *mAU*, milliabsorbance units.

and 11 exons on the minus strand of chromosome 2 (Fig. 1*C*). The 3-kbp cDNA of the human RetSat protein (accession number gi31377747) encodes a protein of 65 kDa, based on theoretical mass calculations of the translated sequence. There is an in-frame stop codon 54 bp upstream of the potential translation initiation site without intervening splice acceptors, which indicates that the 5′-end of the cDNA matches the amino terminus of the protein.

A putative dinucleotide-binding domain (40), also observed in a protein superfamily that includes FAD-binding mammalian monoamine oxidases and protoporphyrinogen oxidases as well as phytoene desaturases (41), is located at the N-terminal portion of RetSat. Another apparent feature is the canonical signal sequence that targets the nascent protein to the membrane of the endoplasmic reticulum (ER) (42). The hydrophobic stretch from residue 568 to 588 is the most likely transmembrane domain.

The cDNA for mouse and macaque monkey RetSat orthologous proteins was cloned from reverse transcribed RNA from the retina and RPE. Sequencing of several independent clones ensured that the sequence was verified. The sequence of the submitted mouse RetSat cDNA (AY704159) has five bases that are different from the sequence available in the data base (gi18483252), two of which result in amino acid changes. In a previous study, rat RetSat expression and other gene products were identified as down-regulated in rat mammary adenocarcinomas, and the rat cDNA was tentatively designated rat mammary tumor-7 (43). No further biochemical characterization of the enzyme was carried out. The sequence we deposited to GenBank™ for mouse RetSat (AY704159) corresponds perfectly to multiple expressed sequence tag sequences, and it is more similar to human RetSat than the sequence currently available in the data base. Monkey RetSat protein (GenBank™ submission AY707524) has 97% con-

served substitutions, including 94% identical residues with the human protein sequence available in the data base (gi46329587).

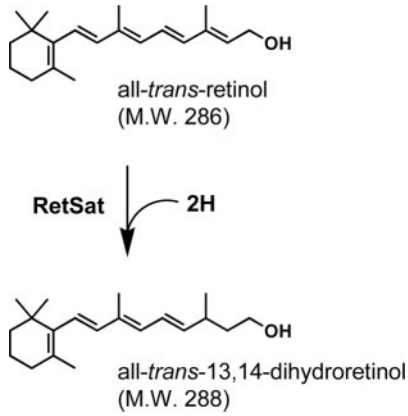

SCHEME 3. **Reaction catalyzed by RetSat converting all-*trans*-retinol into all-*trans*-13,14-dihydroretinol.**

Characterization of the Tissue Distribution and Subcellular Localization of Mouse RetSat Protein—Mouse RetSat expression was examined by Northern blot analysis using a radiolabeled antisense RetSat probe and a commercially available premade blot containing equal amounts of RNA from various tissues. RetSat mRNA appears as a 2200-bp transcript expressed predominantly in the liver and kidney among the tissues examined (Fig. 1*D*, *a*, *top panel*). We also examined the expression of the 2100-bp nonmuscle β-actin mRNA in the same tissues to verify the quality of the RNA on the blot (44) (Fig. 1*D*, *a*, *bottom panel*). Greater amounts of RNA from spleen and lung tissues are present, based on the level of actin detected. Despite this, RetSat mRNA cannot be detected in the corresponding lanes of spleen and lung in the *top panel* of Fig. 1*D* (*a*), whereas it is clearly present in the kidney and liver at the same exposure of the blot (30 min). Very low levels of RetSat were detectable only after much longer exposure of the blot (5 h) in other tissues besides kidney and liver. This was confirmed by reverse transcription-PCR, indicating that RetSat is expressed predominantly in the kidney and liver and at very low levels in many other tissues examined (not shown). A

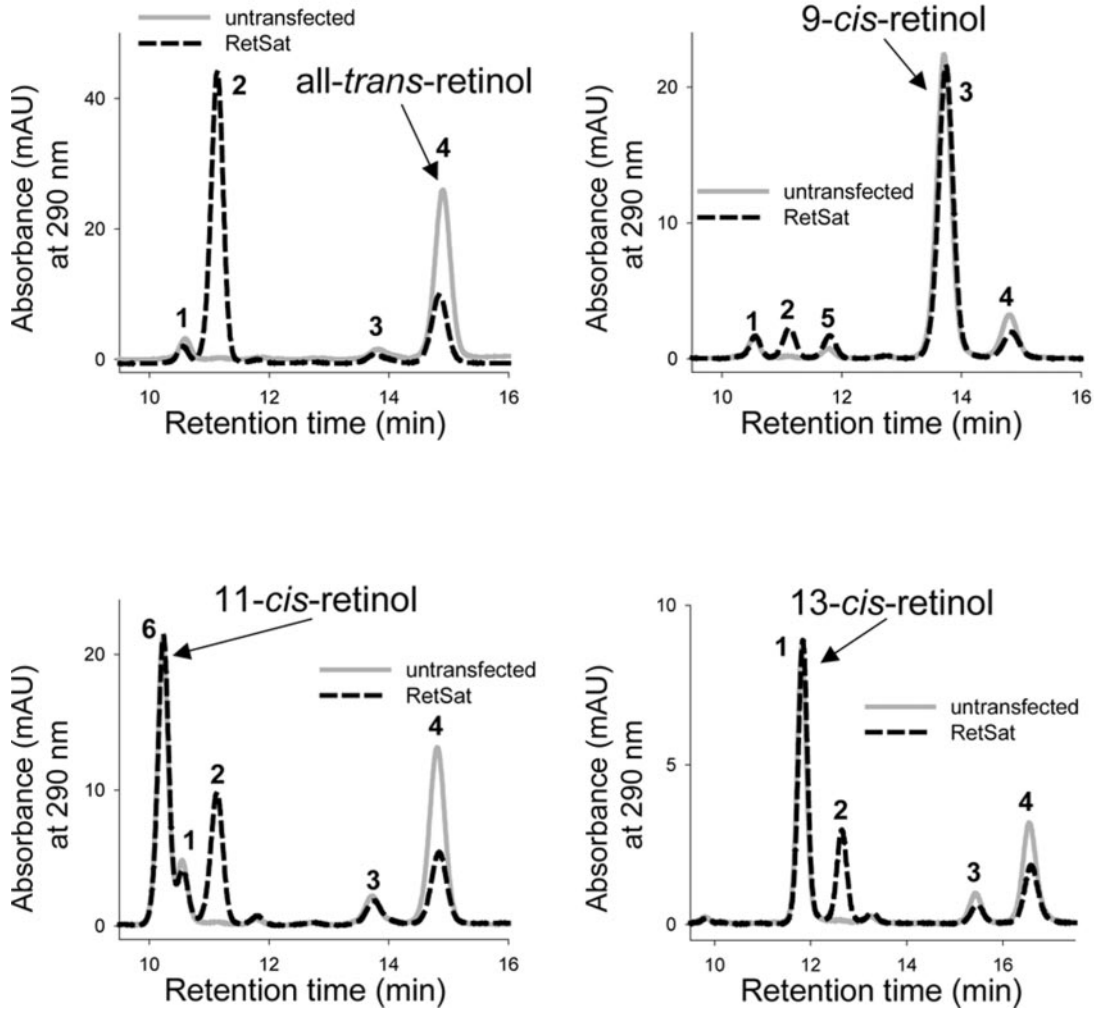

FIG. 5. **Isomeric form of the substrate of mouse RetSat.** Tet-induced HEKK-RetSat cells were incubated overnight with pure isomers of retinol (>95% pure by HPLC, assayed before incubation). Following incubation, retinoids were extracted and analyzed by normal phase HPLC. The appearance of 13,14-dihydroretinol isomers was monitored at 290 nm, since the absorbance maxima of most isomers of 13,14-dihydroretinol differ by less than 5 nm from 290 nm, the λ_{max} of all-*trans*-13,14-dihydroretinol (spectra not shown). In each *panel* an *arrow* indicates the substrate investigated to distinguish it from the additional retinol isomers that were generated by thermal isomerization during overnight incubation in tissue culture. The *numbers* indicate the identity of eluted peaks based on absorbance spectra and comparison with pure standards, specifically 13-*cis*-retinol (*1*), all-*trans*-13,14-dihydroretinol (*2*), 9-*cis*-retinol (*3*), all-*trans*-retinol (*4*), 9,13-di-*cis*-retinol (*5*), and 11-*cis*-retinol (*6*). No isomers of 13,14-dihydroretinol were detected other than the all-*trans* isomer. The retention times in the *bottom right panel* are slightly longer due to variations in the solvent system. The experiment was performed in triplicate and repeated.

rabbit polyclonal antiserum and a monoclonal antibody were prepared against recombinant mouse RetSat. For both mice and rabbit immunogens, a bacterially expressed fragment of the mouse RetSat protein was used as antigen. The recombinant protein fragment was chosen to eliminate the putative dinucleotide-binding domain that may result in cross-reaction with related proteins. Glycosylation-deficient HEK cells obtained from Dr. Khorana (45), HEKK, were transfected with the *tetR* gene and mouse RetSat cDNA under the control of the tetracycline (Tet)-inducible promoter. Stable clones of transfected cells were selected, pooled, and used for further analysis. These cells were designated HEKK-RetSat. Both polyclonal (Fig. 1*D*, *b*) and monoclonal antibodies (Fig. 2*D*) reacted with a specific protein of 70 kDa, similar to the predicted mass of mouse RetSat protein and identical to the mass of the protein detected in Tet-induced HEKK-RetSat cells. Equal amounts of protein from several tissues were analyzed by SDS-PAGE and immunoblotting with anti-RetSat polyclonal antibody. RetSat protein was detected in many tissues, with the highest expression in liver, kidney, and intestine (Fig. 1*D*, *b*). This expression pattern was also confirmed by immunoblotting with the monoclonal anti-RetSat antibody (not shown).

The subcellular localization of mouse RetSat protein was studied by immunocytochemistry using the anti-RetSat monoclonal antibody. First, the antibody was tested for its specificity by staining Tet-induced HEKK-RetSat cells and untransfected cells, which showed no reaction with the antibody (Fig. 2, *A* and *B*). The staining of HEKK-RetSat cells matches that of the perinuclear and ER membrane, indicating that mouse RetSat is targeted to the ER compartment in transfected cells (Fig. 2*C*). There is no cytoplasmic or plasma membrane staining. Subcellular fractionation confirmed that RetSat was a membrane-associated protein not detectable by immunoblotting of the cytosolic supernatant of mouse liver cells with monoclonal antibody (Fig. 2*D*). A protein that migrates with an apparent molecular mass of 70 kDa was seen in both liver microsomal membranes and HEKK-RetSat lysate (Fig. 2*D*). This protein was absent in the lysate of untransfected cells using either RetSat monoclonal antibody or polyclonal anti-RetSat antiserum (not shown).

Tomato CRTISO and Mouse RetSat Exhibit Different Enzyme Activities—Tomato CRTISO was cloned from RNA isolated from the skin and pulp of a fresh red tomato fruit. Tomato CRTISO was expressed in HEKK cells under the control of an inducible promoter. The natural substrate of tomato CRTISO, (7*Z*,9*Z*,9′*Z*,7′*Z*)-tetra-*cis*-lycopene, was isolated by organic extraction of a tangerine tomato, which accumulates (7*Z*,9*Z*,9′*Z*,7′*Z*)-tetra-*cis*-lycopene (32). The tangerine tomato extract consisted mostly of (7*Z*,9*Z*,9′*Z*,7′*Z*)-tetra-*cis*-lycopene (greater than 90%) as determined by reverse-phase HPLC analysis and the UV absorbance spectrum of the main peak, which matched published spectra (*peak S* in Fig. 3*A*, *a*). The (7*Z*,9*Z*,9′*Z*,7′*Z*)-tetra-*cis*-lycopene exhibits a shifted absorbance maxima λ_{max} of 440 nm compared with all-*trans*-lycopene λ_{max} of 475 nm and has a distinct UV absorbance spectrum (46). Untransfected HEKK, RetSat- and CRTISO-expressing cells were incubated in the presence of (7*Z*,9*Z*,9′*Z*,7′*Z*)-tetra-*cis*-lycopene in the dark (Fig. 3*A*). The products of the reaction were analyzed by a reverse-phase HPLC System I. There was no difference in the profile of eluted carotenoids from either untransfected cells or RetSat-expressing cells (Fig. 3*A*, *a* and *b*). As expected, CRTISO-expressing cells converted the substrate (7*Z*,9*Z*,9′*Z*,7′*Z*)-tetra-*cis*-lycopene (*peak S* in Fig. 3*A*, *c*) into all-*trans*-lycopene, with a λ_{max} of 475 nm (*P* in Fig. 3*A*, *c*). All-*trans*-lycopene was identified based on its absorbance spectrum and co-elution with an available standard obtained from

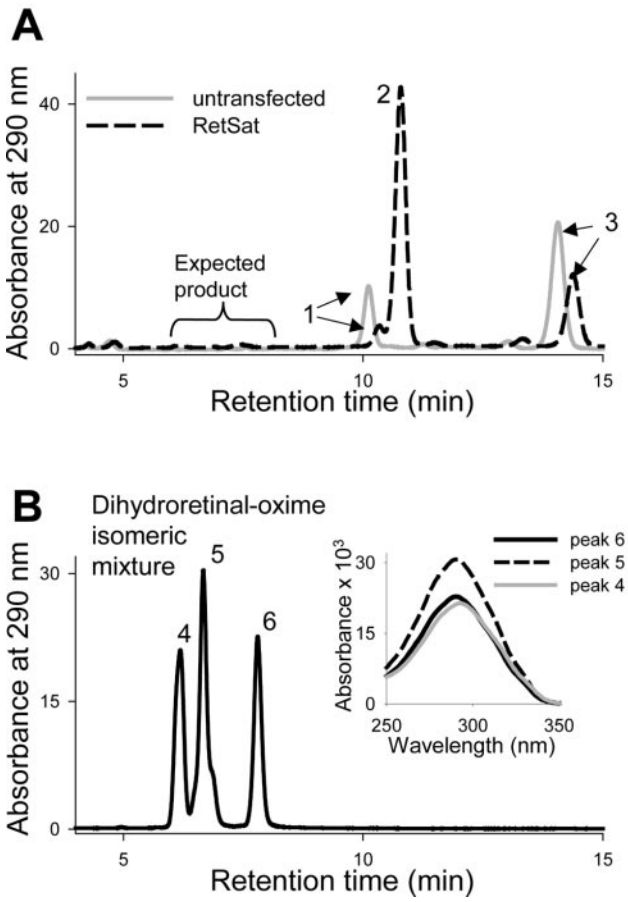

FIG. 6. **RetSat activity toward all-*trans*-retinal.** *A*, analysis of retinal conversion in RetSat-expressing cells. Tet-induced HEKK-RetSat or untransfected cells were incubated overnight with pure all-*trans*-retinal (>99% pure by HPLC, assayed before incubation). Following incubation, retinals were derivatized with hydroxylamine, extracted, and analyzed by normal phase HPLC. The appearance of *syn*- and *anti*-oximes of 13,14-dihydroretinal was monitored at 290 nm (expected 6–8 min after injection, as indicated). The *peak numbers* represent 13-*cis*-retinol (*1*), all-*trans*-13,14-dihydroretinol (*2*), and all-*trans*-retinol (*3*). *B*, synthetic standards of 13,14-dihydroretinal derivatized with hydroxylamine were examined by normal phase HPLC in order to establish product elution profile. The *inset* shows the spectra of the different isomers of 13,14-dihydroretinal-oximes.

Dr. Kurt Bernhard (CaroteNature GmbH, Lupsingen, Switzerland) and Dr. Regina Goralczyk (Roche Vitamins Ltd., Basel, Switzerland). CRTISO also catalyzed the conversion of (7*Z*,9*Z*,9′*Z*,7′*Z*)-tetra-*cis*-lycopene into a compound labeled *1* in Fig. 3*A*, which we tentatively identified as a 7,9-di-*cis*-lycopene isomer based on its absorbance spectrum (46). This observation would suggest a two-step reaction mechanism for CRTISO, in which both *cis*-bonds of first one end and then the other of the carotenoid are isomerized. Thermally induced or light-induced isomerization can convert (7*Z*,9*Z*,9′*Z*,7′*Z*)-tetra-*cis*-lycopene into the (7*Z*,9*Z*)-di-*cis*-isomer at a slower rate, since this compound was also present in the original tomato extract (*peak 1* in Fig. 3*A*, *a* and *b*) and reported by other investigators (47).

Our analysis of various carotenoid and retinoid substrates led us to investigate the activity of RetSat in the presence of all-*trans*-retinol. When the products of the reaction were examined by normal phase HPLC, we noticed that RetSat-expressing cells incubated with all-*trans*-retinol (*peak S* in Fig. 3*B*) in the dark converted it to a less polar compound whose λ_{max} was 290 nm (*peak P* in Fig. 3*B*, *b*). The peak was absent in untransfected and CRTISO-expressing cells. *cis*-Isomers of retinol (*peaks 2–4* in Fig. 3*B*) generated during the overnight incubation were present in all cells regardless of background. Based

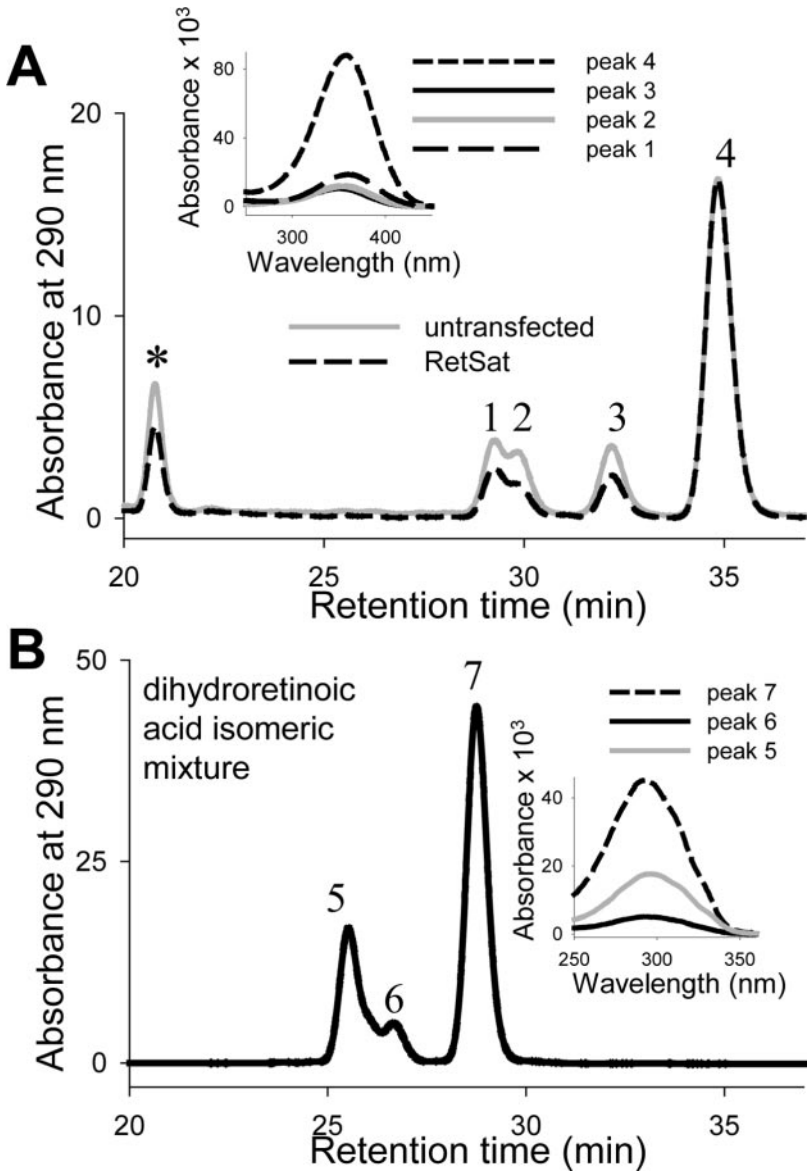

FIG. 7. **RetSat activity toward all-*trans*-retinoic acid.** *A*, analysis of retinoic acid conversion in RetSat-expressing cells. Tet-induced HEKK-RetSat or untransfected cells were incubated overnight with pure all-*trans*-retinoic acid (>90% pure by HPLC, assayed before incubation). Following incubation, retinoic acid was extracted and analyzed by reverse-phase HPLC System II. The appearance of 13,14-dihydroretinoic acid isomers was monitored at 290 nm (expected 25–30 min after injection). The *peak numbers* represent 13-*cis*-retinoic acid (*1*), 9,13-di-*cis*-retinoic acid (*2*), 9-*cis*-retinoic acid (*3*), and all-*trans*-retinoic acid (*4*). *B*, mixture of isomers of synthetic standards of 13,14-dihydroretinoic acid were examined by reverse-phase HPLC System II in order to establish the product elution profile. The *inset* shows the spectra of the different isomers of 13,14-dihydroretinoic acid. *, an unrelated compound. The experiment was performed in triplicate samples and repeated.

on the hypsochromic-shifted UV absorbance maximum of 290 nm, we deduced that the new compound has one fewer double bond as compared with the parent compound retinol exhibiting a λ_{max} of 325 nm. A survey of the literature indicates that all-*trans*-13,14-dihydroretinal exhibits a maximum absorption at 289 nm (48). To prove the hypothesis that the unknown compound is all-*trans*-13,14-dihydroretinol, it was chemically synthesized as depicted in Scheme 2, purified by HPLC, and characterized by ^{1}H NMR spectrum. The unknown compound produced by RetSat-expressing cells was purified by collecting the appropriate fraction from a normal phase HPLC. The purity of the unknown biosynthetic compound and synthetic all-*trans*-13,14-dihydroretinol was verified by normal phase HPLC (Fig. 4*A*, *a* and *b*). The amount of the purified unknown compound precluded us from conducting its ^{1}H NMR analysis. However, both all-*trans*-13,14-dihydroretinol and the unknown compound exhibit the same chromatographic properties on normal phase HPLC, since they co-eluted as one peak when combined (Fig. 4*A*, *c*). The two compounds have identical UV absorbance spectra (Fig. 4*B*), and light-induced isomerization of equal amounts of the two compounds generates a series of *cis*-isomers identical in both elution profile and intensity (Fig. 4*C*). Acetylation of the synthetic all-*trans*-13,14-dihydroretinol and the extracted compounds produced ester compounds that co-eluted on a normal phase HPLC (data not shown). More importantly, MS analysis revealed that the biosynthetic compound has an *m/z* mass of 288, an increase of 2 daltons from the mass of the parent compound, all-*trans*-retinol (*m/z* = 286) (Fig. 4*D*, *a*, *inset*). This observed mass is the same as the mass of synthetic all-*trans*-13,14-dihydroretinol (Fig. 4*D*, *b*, *inset*). The MS fragmentation pattern of the both synthetic and biosynthetic compounds is identical (Fig. 4*D*, *a* and *b*). Since C13 becomes a chiral center in 13,14-dihydroretinol, further NMR analysis will be necessary to establish the absolute configuration of the biosynthetic compound. These findings lead us to propose that RetSat catalyzed the saturation reaction of the 13–14 double bond of all-*trans*-retinol as depicted in Scheme 3.

Substrate Selectivity of Mouse RetSat—The substrate specificity of RetSat was investigated using purified isomers of retinol. RetSat-expressing cells were incubated overnight with the different retinol isomers. The isomers were more than 95% pure at the time of the addition as confirmed by normal phase HPLC analysis. However, during the overnight incubation, *cis*-isomers of retinol converted to all-*trans* isomer and then back to other *cis*-retinol isomers, complicating the interpretation of results. All-*trans*-retinol was clearly a good substrate for RetSat based on the amount of all-*trans*-13,14-dihydroretinol produced (*peak 2* in Fig. 5, *top left*) and the amount of all-*trans*-retinol utilized (*peak*

4 in Fig. 5, *solid gray* and *short dashed black trace* representing untransfected and RetSat-expressing cells, respectively). Only all-*trans*-13,14-dihydroretinol product was formed in all reactions, and no *cis*-isomers were detected. In all assays with *cis*-retinol isomers, the amount of all-*trans*-13,14-dihydroretinol produced correlates with the amount of all-*trans*-retinol present and utilized in the reaction. Meanwhile, the amount of *cis*-retinol substrate stayed the same in either RetSat-expressing (*short dashed black trace*) or untransfected cells (*solid gray trace* in Fig. 5). Based on this evidence, it appears that all-*trans*-retinol was the preferred substrate for RetSat. The all-*trans*-13,14-dihydroretinol found in cells incubated with *cis*-retinol isomers was produced from all-*trans*-retinol derived by spontaneous isomerization of the *cis*-retinol substrate.

We also examined whether retinal or retinoic acid could be saturated by RetSat to corresponding 13,14-dihydroretinal or 13,14-dihydroretinoic acid. Retinal was almost completely reduced to retinol by incubation with cells as evident by the barely detectable levels of retinal-oximes and the appearance of retinol (*peak 3* in Fig. 6*A*). In RetSat-expressing cells, all-*trans*-retinol was then readily converted to all-*trans*-13,14-dihydroretinol (*peak 2* in Fig. 6*A*). Synthetic 13,14-dihydroretinal-oxime derivatives (λ_{max} = 290 nm) were examined on the same HPLC system to establish product elution conditions (Fig. 6*B* and *inset spectra*). However, no dihydroretinal-oximes were detected in RetSat-expressing cells incubated with retinal (6–8-min elution time) (Fig. 6*A*). It was not possible to conclusively establish whether retinal is a substrate for RetSat given the rapid conversion of retinal to retinol in cultured cells.

Incubation of cells with retinoic acid indicated that it is not a substrate for saturation by RetSat (Fig. 7*A*). Synthetic 13–14-dihydroretinoic acid standards were examined on the same HPLC system to establish their elution conditions (Fig. 7*B*). Although 13-*cis*-retinoic acid (*peak 1* in Fig. 7*A*) coelutes with all-*trans*-13,14-dihydroretinoic (*peak 7* in Fig. 7*B*), the absorbance spectrum of the two compounds is different (Fig. 7, *A* and *B*, *insets*) and allowed us to conclude that 13,14-dihydroretinoic acid cannot be detected in RetSat-expressing cells incubated with retinoic acid.

To avoid thermal isomerization, the substrates were examined in homogenized microsomal RetSat membranes with or without additional cofactors. Membrane homogenate from RetSat-expressing cells was incubated with all-*trans*-retinol, and the product of the reaction was examined by normal phase HPLC. There was little all-*trans*-13,14-dihydroretinol produced, as indicated by the elution peak labeled *2*, *solid black trace*, Fig. 8. The addition of reduced dinucleotide cofactors NADH or NADPH had no effect on the yield of the reaction (not shown). For control, membranes from untransfected cells (*gray trace*) and boiled membranes from RetSat-expressing cells (*short dashed black trace*) showed no activity. Cell homogenization destroyed the activity of RetSat most likely by affecting the redox status or by the loss of a key cofactor. The low activity of RetSat *in vitro* is not surprising given the well documented labile nature of CRTISO (27) and phytoene desaturase enzymes (49).

All-trans-13,14-dihydroretinol Can Be Detected in Several Tissues of Animals Maintained on a Normal Diet—The presence of RetSat in major organs such as the liver and kidney led us to investigate whether all-*trans*-13,14-dihydroretinol could be detected in tissues. All-*trans*-13,14-dihydroretinol could be readily detected by normal phase HPLC analysis of mouse liver and kidney and bovine retina and RPE (Fig. 9). All-*trans*-13,14-dihydroretinol was recognized based on its UV absorbance spectrum and chromatographic retention time, which both matched those of the synthetic compound. Retinol isomers such as 13-*cis*-retinol (*peak 1*), 9,13-di-*cis*-retinol (*peak 2*), all-*trans*-retinol (*peak 3*), and 11-*cis*-retinol (*peak 4*) (Fig. 9) were also detected and recognized based on available standards and UV absorbance maxima. We conclude that all-*trans*-13,14-dihydroretinol represents a minor but readily detectable retinoid in many tissues examined from animals maintained on a normal diet not supplemented with vitamin A.

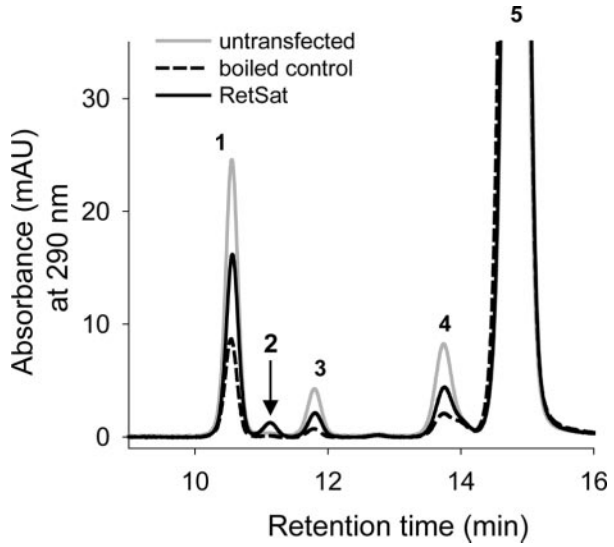

FIG. 8. **RetSat activity in homogenized cells.** Untransfected cells (*solid gray trace*) or Tet-induced HEKK-RetSat cells (*solid black trace*) were homogenized and incubated with all-*trans*-retinol substrate, followed by retinoid extraction and normal phase HPLC analysis. The elution profile was monitored at 290 nm for the appearance of all-*trans*-13,14-dihydroretinol. In control samples (*short dashed black trace*) cell homogenate from HEKK-RetSat cells was boiled 10 min at 95 °C prior to incubation with substrate. The addition of 0.4 mM NADH or NADPH had no effect on the yield of all-*trans*-13,14-dihydroretinol. The experiment was performed in duplicate. The *peak numbers* represent 13-*cis*-retinol (*1*), all-*trans*-13,14-dihydroretinol (*2*), 9,13-di-*cis*-retinol (*3*), 9-*cis*-retinol (*4*), and all-*trans*-retinol (*5*). *mAU*, milliabsorbance units.

Esterification of All-trans-13,14-dihydroretinol in RPE Microsomes and HEKK-LRAT Cells—LRAT converts all-*trans*-retinol to all-*trans*-retinyl esters, thereby controlling its availability and absorption (1, 2). To better understand the metabolism of all-*trans*-13,14-dihydroretinol, we assayed whether it could be esterified by LRAT present in RPE or expressed in transfected cells according to previously published procedures (4). We found that all-*trans*-13,14-dihydroretinol was as good a substrate for LRAT as all-*trans*-retinol by being converted to all-*trans*-13,14-dihydroretinyl esters (Fig. 10). This is in agreement with the esterification of all-*trans*-13,14-dihydroretinol by amphibian RPE (50). From this, we conclude that esterification may be a metabolic/storage pathway for all-*trans*-13,14-dihydroretinol, which will have to be confirmed *in vivo*.

DISCUSSION

The findings presented in this report suggest that we uncovered a novel and potentially important pathway in the metabolism of vitamin A. RetSat, a novel enzyme, catalyzes a brand new activity, the saturation of the 13–14 double bond of all-*trans*-retinol. The product of the RetSat reaction, all-*trans*-13,14-dihydroretinol, was detected for the first time *in vivo*. The all-*trans*-13,14-dihydroretinol metabolite may be bioactive or may lead to other bioactive compounds; alternatively, it may be part of a catabolic pathway. Now that the enzyme and reaction have been identified, altering the activity of RetSat will allow us to investigate its role and that of all-*trans*-13,14-dihydroretinol *in vivo*.

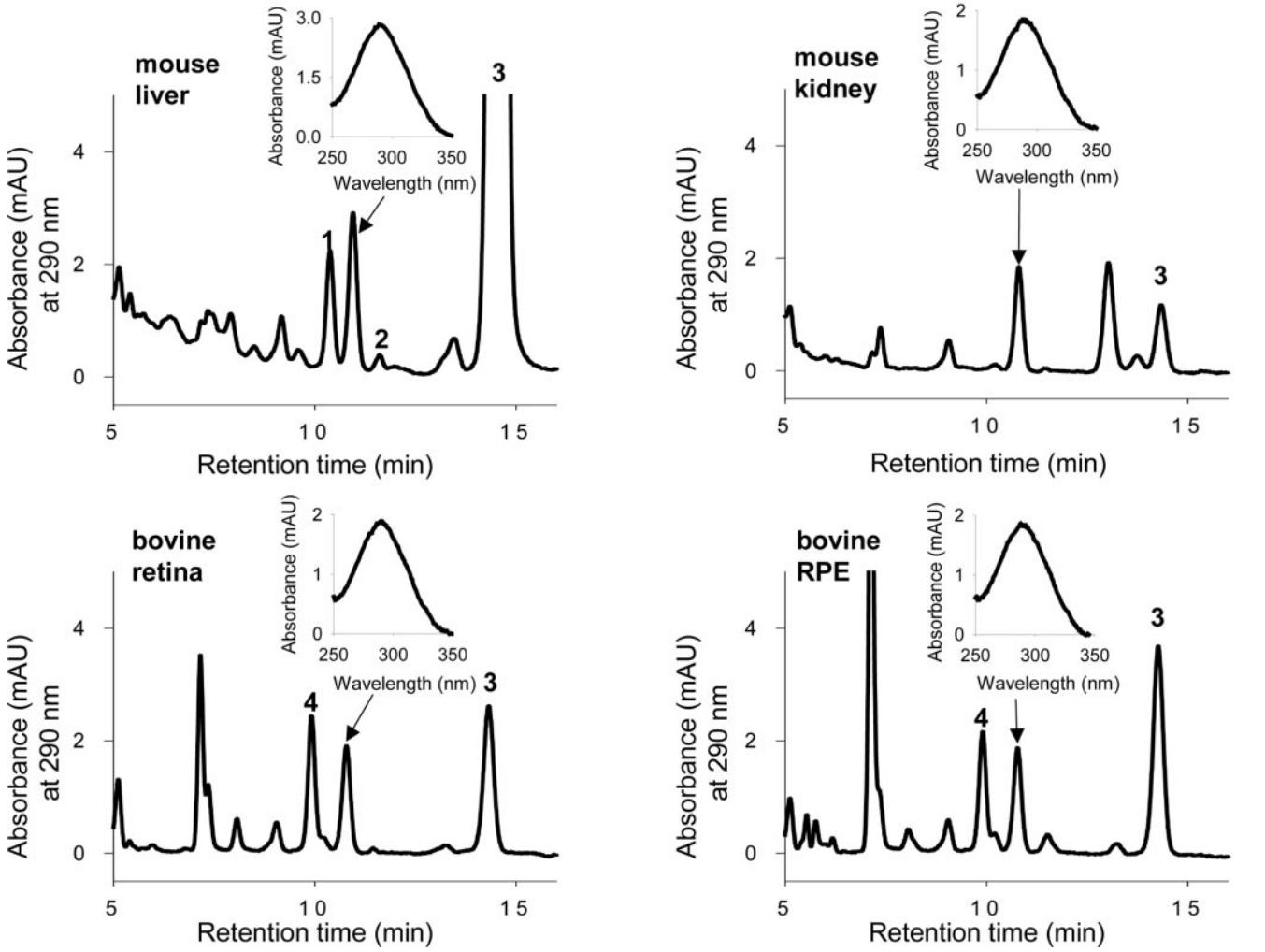

FIG. 9. **Identification of all-*trans*-13,14-dihydroretinol in various tissues.** Retinoids were extracted from mouse liver (0.3 g, *top left panel*), kidney (0.2 g, *top right panel*), bovine retina (0.2 g, *bottom left panel*), and RPE (0.2 g, *bottom right panel*) and examined by normal phase HPLC. The elution of 13,14-dihydroretinol was monitored at 290 nm. Based on its retention time and absorbance spectrum, a peak corresponding to all-*trans*-13,14-dihydroretinol was identified in all tissues examined; it elutes on normal phase HPLC between 13-*cis*-retinol (*1*) and 9,13-di-*cis*-retinol (*2*). Other peaks corresponding to all-*trans*-retinol (*3*) and 11-*cis*-retinol (*4*; bovine retina and RPE) were also identified. The experiment was performed in duplicate from tissues of different animals. The yield of all-*trans*-13,14-dihydroretinol was slightly higher (<10%) by saponification of the extract before HPLC analysis. *mAU*, milliabsorbance units.

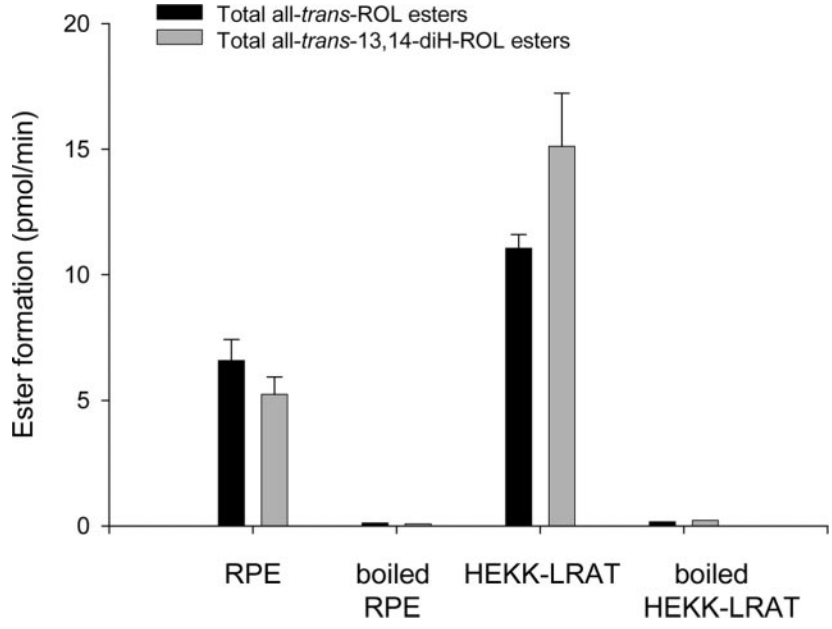

FIG. 10. **LRAT activity.** Two nmol of retinols were incubated with RPE microsomes and with homogenized HEKK-LRAT cells for 10 min. The production of esters was monitored by HPLC measuring absorbance at 325 nm for all-*trans*-retinol (*black bars*) and 290 nm for all-*trans*-14,13-dihydroretinol (*gray bars*). Protein concentrations were not equalized. No activity was observed in controls with protein boiled for 10 min at 95 °C. Experiments were performed in triplicate.

Vertebrate (13,14)-All-trans-retinol Saturase: An Ancient Enzyme—In addition to RetSat, enzymes involved in retinoid processing such as retinal dehydrogenase and CYP26 and one retinoic acid receptor can be found in the translation of the draft genomic sequence of the primitive chordates, the ascidians *C. intestinalis* and *C. savignyi* (51). The ascidian tadpole-larva contains a notochord and a dorsal tubular nerve cord much like a vertebrate tadpole and is considered a good approximation of the chordate ancestor. The acquisition of the anterioposterior organized body plan in chordates coincides with the innovation of RA and its nuclear receptor to control development. No retinoic acid receptors have so far been found in nonchordate species (52). Identification of a putative ascidian RetSat underscores the potential importance of the pathway that starts with the saturation of the 13–14 double bond of retinol. As retinoid metabolism evolved, chordate metabolism modified an existing enzyme, possibly an ancient phytoene desaturase, in order to create new metabolites with novel functions.

Carotenoid- and retinoid-modifying enzymes share many features determined by the highly related nature of their substrates. The 9-*cis*-neoxanthin cleavage enzyme from plants, VP14, is similar to β,β-carotene-oxygenases BCO-I and -II from flies, *ninaB*, and vertebrates (22). Another vertebrate protein related to carotenoid cleavage enzymes is RPE65, which is essential for the production of 11-*cis*-retinol, a key step of the visual cycle (53). The function of RPE65 is not clear, since it was shown to bind retinyl esters (54), yet no catalytic role has been ascribed to it. In vertebrates, P450 enzymes CYP26A1 and -B1 convert retinoic acid (a diterpenoid) to hydroxylated metabolites (15, 17). Closely related P450 enzymes from plants hydroxylate abscisic acid, a sesquiterpene hormone that controls the plant life cycle, and taxol, a plant diterpenoid (55, 56). Based on its activity, RetSat is a retinoid-saturating enzyme related to carotenoid desaturases (phytoene desaturase, ζ-carotene desaturase, and CrtI), whereas the primary amino acid sequence relates to CRTISO.

Structural Analysis of the RetSat Enzyme—Sequence analysis of the vertebrate RetSat family proteins reveals a dinucleotide-binding motif (40, 57), $U_4G(G/A)GUXGLX_2(A/S)X_2L(X_{6-12})UX(L/V)UE(X_4)UGG(X_{9-13})(G/V)X_3(D/E)XG$, where U is a hydrophobic residue and *X* is any residue. Many proteins with this motif, including monoamine oxidases, protoporphyrinogen oxidases, and many phytoene desaturases, have been shown to be stimulated by FAD (58, 59), and others have been shown to be stimulated by NAD or NADP (60). The presence of a putative dinucleotide-binding motif in the sequence of RetSat argues that saturation of the double bond occurs through the transfer of a hydride (H^-) ion from a reduced cofactor (NAD(P)H or $FADH_2$) and a proton from the solution. This may explain the labile nature of RetSat in homogenized cells (*i.e.* cells in which the redox state has been altered).

We show that mouse RetSat is membrane-associated and appears to localize to the ER compartment of transfected cells. A cleavable signal sequence can be readily identified at the amino terminus of the protein, indicating that the protein is targeted to the ER membrane. In addition, a stretch of hydrophobic amino acids from residue 568 to 588 is a strong candidate for a transmembrane domain.

13,14-Dihydroretinols in Biological Systems—Retinoids containing saturated 13–14 double bonds such as 9-*cis*-13,14-dihydroretinoic acid and its taurine conjugate (61), 9-*cis*-4-oxo-13,14-dihydroretinoic acid (62), were previously identified in animals supplemented with 9-*cis*-retinoic acid or retinyl palmitate, respectively. Another saturated all-*trans*-13,14-dihydroxy-retinol was detected in retinol-treated lymphoblastoma 5/2 cells and was shown to support the proliferation of lymphocytes (63). The RetSat-catalyzed saturation reaction prefers all-*trans*-retinol as a substrate, which leads to specific synthesis of all-*trans*-13,14-dihydroretinol. Here we show that all-*trans*-13,14-dihydroretinol is detectable in unsupplemented animals (Fig. 9). It is preferable to demonstrate the existence of metabolite *in vivo* in animals maintained on a normal diet or receiving physiological levels of labeled precursor. This is the first report of this retinoid *in vivo*. Future studies will examine whether all-*trans*-13,14-dihydroretinol has biological activity or is metabolized to other active compounds. Although it is possible that all-*trans*-13,14-dihydroretinol is a breakdown product of all-*trans*-retinol, we find this unlikely, since retinol and retinoic acid are degraded through oxidation to polar catabolites. The precise role of all-*trans*-13,14-dihydroretinol *in vivo* remains to be established.

Is All-trans-13,14-dihydroretinol on the Pathway for the Degradation or Formation of All-trans-13,14-dihydroretinoic Acid?—The 13,14-dihydroretinoic acid and its catabolic product 4-oxo-13,14-dihydroretinoic acid have been previously identified in supplemented animals (61, 62). The 13,14-dihydroretinoic acid can be formed by oxidation of 13,14-dihydroretinol or by saturation of the 13–14 double bond of retinoic acid. In our assay system, RetSat cannot convert all-*trans*-retinoic acid into all-*trans*-13,14-dihydroretinoic acid, which implies that that the previously observed metabolites are downstream products of the oxidation of all-*trans*-13,14-dihydroretinol. The oxidation of all-*trans*-13,14-dihydroretinol most likely employs the same enzymes as all-*trans*-retinol, members of the short-chain alcohol dehydrogenase family or of the medium-chain alcohol dehydrogenase family, to generate all-*trans*-13,14-dihydroretinal and retinal dehydrogenase 1, 2, or 3 to further generate all-*trans*-13,14-dihydroretinoic acid. Given that previously observed metabolites were in 9-*cis* conformation, it is unclear at what stage 9–10 bond isomerization occurs and whether this reaction is enzymatic.

Relationship between Plant and Vertebrate Enzymes: A Productive Pathway of Discovery—Carotenoids and retinoids play essential roles in biology. Their unique light-absorbing properties allow carotenoids to mediate photosynthesis and photoprotection and allow retinoids to form the visual chromophore. Through metabolites they can also regulate gene expression as seen for abscisic and retinoic acid. The only natural source of carotenoids, and hence retinoids, are plants and photosynthetic bacteria. Although vertebrates do not synthesize carotenoids or retinoids, they are able to transform them to generate a unique series of metabolites. Vertebrate enzymes involved in carotenoid and retinoid processing probably evolved by changing the substrate of an existing terpenoid modifying enzyme or by reactivating an ancestral gene inherited from a common ancestor of animals, plants, and photosynthetic bacteria. Studying the relationship between plant and vertebrate enzymes is a productive pathway of discovery. Both carotenoid and retinoid biochemistry can gain a new level of understanding through cross-fertilization of the two fields.

Acknowledgments—We thank Dr. Jing Huang for help with the monoclonal antibody production, Dr. Martin Sadilek for recording the electron impact mass spectrometry spectra of all-*trans*-13,14-dihydroretinol, and Dr. Josh McBee for analyzing recombinant RetSat by liquid chromatography-MS. We are grateful to Dr. Michael Gelb for providing facilities for the chemical synthesis. We also thank Dr. Gobind Khorana for providing glycosylation-deficient HEK293S cells and Dr. Kurt Bernhard and Dr. Regina Goralczyk for providing carotenoid standards. We thank Dr. Johannes von Lintig and Dr. Marcin Golczak for insightful comments and Rebecca Birdsong for proofreading the manuscript.

REFERENCES

1. Ruiz, A., Winston, A., Lim, Y. H., Gilbert, B. A., Rando, R. R., and Bok, D. (1999) *J. Biol. Chem.* **274,** 3834–3841
2. Batten, M. L., Imanishi, Y., Maeda, T., Tu, D. C., Moise, A. R., Bronson, D.,

Possin, D., Van Gelder, R. N., Baehr, W., and Palczewski, K. (2004) *J. Biol. Chem.* **279,** 10422–10432
3. Imanishi, Y., Batten, M. L., Piston, D. W., Baehr, W., and Palczewski, K. (2004) *J. Cell Biol.* **164,** 373–383
4. Kuksa, V., Imanishi, Y., Batten, M., Palczewski, K., and Moise, A. R. (2003) *Vision Res.* **43,** 2959–2981
5. Chou, C. F., Lai, C. L., Chang, Y. C., Duester, G., and Yin, S. J. (2002) *J. Biol. Chem.* **277,** 25209–25216
6. Duester, G. (2000) *Eur. J. Biochem.* **267,** 4315–4324
7. Bhat, P. V., Labrecque, J., Boutin, J. M., Lacroix, A., and Yoshida, A. (1995) *Gene* (*Amst.*) **166,** 303–306
8. Penzes, P., Wang, X., Sperkova, Z., and Napoli, J. L. (1997) *Gene* (*Amst.*) **191,** 167–172
9. Wang, X., Penzes, P., and Napoli, J. L. (1996) *J. Biol. Chem.* **271,** 16288–16293
10. Zhao, D., McCaffery, P., Ivins, K. J., Neve, R. L., Hogan, P., Chin, W. W., and Drager, U. C. (1996) *Eur. J. Biochem.* **240,** 15–22
11. Mic, F. A., Molotkov, A., Fan, X., Cuenca, A. E., and Duester, G. (2000) *Mech. Dev.* **97,** 227–230
12. Lin, M., Zhang, M., Abraham, M., Smith, S. M., and Napoli, J. L. (2003) *J. Biol. Chem.* **278,** 9856–9861
13. Chambon, P. (1996) *FASEB J.* **10,** 940–954
14. Taimi, M., Helvig, C., Wisniewski, J., Ramshaw, H., White, J., Amad, M., Korczak, B., and Petkovich, M. (2004) *J. Biol. Chem.* **279,** 77–85
15. Fujii, H., Sato, T., Kaneko, S., Gotoh, O., Fujii-Kuriyama, Y., Osawa, K., Kato, S., and Hamada, H. (1997) *EMBO J.* **16,** 4163–4173
16. White, J. A., Guo, Y. D., Baetz, K., Beckett-Jones, B., Bonasoro, J., Hsu, K. E., Dilworth, F. J., Jones, G., and Petkovich, M. (1996) *J. Biol. Chem.* **271,** 29922–29927
17. White, J. A., Ramshaw, H., Taimi, M., Stangle, W., Zhang, A., Everingham, S., Creighton, S., Tam, S. P., Jones, G., and Petkovich, M. (2000) *Proc. Natl. Acad. Sci. U. S. A.* **97,** 6403–6408
18. Buck, J., Derguini, F., Levi, E., Nakanishi, K., and Hammerling, U. (1991) *Science* **254,** 1654–1656
19. Buck, J., Grun, F., Derguini, F., Chen, Y., Kimura, S., Noy, N., and Hammerling, U. (1993) *J. Exp. Med.* **178,** 675–680
20. von Lintig, J., Dreher, A., Kiefer, C., Wernet, M. F., and Vogt, K. (2001) *Proc. Natl. Acad. Sci. U. S. A.* **98,** 1130–1135
21. Kiefer, C., Hessel, S., Lampert, J. M., Vogt, K., Lederer, M. O., Breithaupt, D. E., and von Lintig, J. (2001) *J. Biol. Chem.* **276,** 14110–14116
22. Giuliano, G., Al-Babili, S., and von Lintig, J. (2003) *Trends Plant Sci.* **8,** 145–149
23. Redmond, T. M., Gentleman, S., Duncan, T., Yu, S., Wiggert, B., Gantt, E., and Cunningham, F. X., Jr. (2001) *J. Biol. Chem.* **276,** 6560–6565
24. Yan, W., Jang, G. F., Haeseleer, F., Esumi, N., Chang, J., Kerrigan, M., Campochiaro, M., Campochiaro, P., Palczewski, K., and Zack, D. J. (2001) *Genomics* **72,** 193–202
25. Snodderly, D. M. (1995) *Am. J. Clin. Nutr.* **62,** 1448S-1461S
26. Fraser, P. D., and Bramley, P. M. (2004) *Prog. Lipid Res.* **43,** 228–265
27. Park, H., Kreunen, S. S., Cuttriss, A. J., DellaPenna, D., and Pogson, B. J. (2002) *Plant Cell* **14,** 321–332
28. Isaacson, T., Ronen, G., Zamir, D., and Hirschberg, J. (2002) *Plant Cell* **14,** 333–342
29. Breitenbach, J., Vioque, A., and Sandmann, G. (2001) *Z. Naturforsch.* **56,** 915–917
30. Masamoto, K., Wada, H., Kaneko, T., and Takaichi, S. (2001) *Plant Cell Physiol.* **42,** 1398–1402
31. Giuliano, G., Giliberto, L., and Rosati, C. (2002) *Trends Plant Sci* **7,** 427–429
32. Zechmeister, L., LeRosen, A. L., Went, F. W., and Pauling, L. (1941) *Proc. Natl. Acad. Sci. U. S. A.* **21,** 468–474
33. Giuliano, G., Pollock, D., and Scolnik, P. A. (1986) *J. Biol. Chem.* **261,** 12925–12929
34. Sandmann, G. (2002) *Physiol. Plant.* **116,** 431–440
35. Haeseleer, F., Jang, G. F., Imanishi, Y., Driessen, C. A., Matsumura, M., Nelson, P. S., and Palczewski, K. (2002) *J. Biol. Chem.* **277,** 45537–45546
36. Adamus, G., Zam, Z. S., Emerson, S. S., and Hargrave, P. A. (1989) *In Vitro Cell Dev. Biol.* **25,** 1141–1146
37. Bradford, M. M. (1976) *Anal. Biochem.* **72,** 248–254
38. Garwin, G. G., and Saari, J. C. (2000) *Methods Enzymol.* **316,** 313–324
39. Stecher, H., Gelb, M. H., Saari, J. C., and Palczewski, K. (1999) *J. Biol. Chem.* **274,** 8577–8585
40. Wierenga, R. K., Terpstra, P., and Hol, W. G. (1986) *J. Mol. Biol.* **187,** 101–107
41. Dailey, T. A., and Dailey, H. A. (1998) *J. Biol. Chem.* **273,** 13658–13662
42. Blobel, G., Walter, P., Chang, C. N., Goldman, B. M., Erickson, A. H., and Lingappa, V. R. (1979) *Symp. Soc. Exp. Biol.* **33,** 9–36
43. Wang, Y., Hu, L., Yao, R., Wang, M., Crist, K. A., Grubbs, C. J., Johanning, G. L., Lubet, R. A., and You, M. (2001) *Oncogene* **20,** 7710–7721
44. Alonso, S., Minty, A., Bourlet, Y., and Buckingham, M. (1986) *J. Mol. Evol.* **23,** 11–22
45. Reeves, P. J., Callewaert, N., Contreras, R., and Khorana, H. G. (2002) *Proc. Natl. Acad. Sci. U. S. A.* **99,** 13419–13424
46. Hengartner, U., Bernhard, K., Meyer, K., Englert, G., and Glinz, E. (1992) *Helv. Chim. Acta* **75,** 1848–1865
47. Bartley, G. E., Scolnik, P. A., and Beyer, P. (1999) *Eur. J. Biochem.* **259,** 396–403
48. Yan, B., Spudich, J. L., Mazur, P., Vunnam, S., Derguini, F., and Nakanishi, K. (1995) *J. Biol. Chem.* **270,** 29668–29670
49. Cunningham, F. X., and Gantt, E. (1998) *Annu. Rev. Plant Physiol. Plant Mol. Biol.* **49,** 557–583
50. Law, W. C., Rando, R. R., Canonica, S., Derguini, F., and Nakanishi, K. (1988) *J. Am. Chem. Soc.* **110,** 5915–5917
51. Dehal, P., Satou, Y., Campbell, R. K., Chapman, J., Degnan, B., De Tomaso, A., Davidson, B., Di Gregorio, A., Gelpke, M., Goodstein, D. M., Harafuji, N., Hastings, K. E., Ho, I., Hotta, K., Huang, W., Kawashima, T., Lemaire, P., Martinez, D., Meinertzhagen, I. A., Necula, S., Nonaka, M., Putnam, N., Rash, S., Saiga, H., Satake, M., Terry, A., Yamada, L., Wang, H. G., Awazu, S., Azumi, K., Boore, J., Branno, M., Chin-Bow, S., DeSantis, R., Doyle, S., Francino, P., Keys, D. N., Haga, S., Hayashi, H., Hino, K., Imai, K. S., Inaba, K., Kano, S., Kobayashi, K., Kobayashi, M., Lee, B. I., Makabe, K. W., Manohar, C., Matassi, G., Medina, M., Mochizuki, Y., Mount, S., Morishita, T., Miura, S., Nakayama, A., Nishizaka, S., Nomoto, H., Ohta, F., Oishi, K., Rigoutsos, I., Sano, M., Sasaki, A., Sasakura, Y., Shoguchi, E., Shin-i, T., Spagnuolo, A., Stainier, D., Suzuki, M. M., Tassy, O., Takatori, N., Tokuoka, M., Yagi, K., Yoshizaki, F., Wada, S., Zhang, C., Hyatt, P. D., Larimer, F., Detter, C., Doggett, N., Glavina, T., Hawkins, T., Richardson, P., Lucas, S., Kohara, Y., Levine, M., Satoh, N., and Rokhsar, D. S. (2002) *Science* **298,** 2157–2167
52. Fujiwara, S., and Kawamura, K. (2003) *Zool. Sci.* **20,** 809–818
53. Redmond, T. M., Yu, S., Lee, E., Bok, D., Hamasaki, D., Chen, N., Goletz, P., Ma, J. X., Crouch, R. K., and Pfeifer, K. (1998) *Nat. Genet.* **20,** 344–351
54. Mata, N. L., Moghrabi, W. N., Lee, J. S., Bui, T. V., Radu, R. A., Horwitz, J., and Travis, G. H. (2004) *J. Biol. Chem.* **279,** 635–643
55. Saito, S., Hirai, N., Matsumoto, C., Ohigashi, H., Ohta, D., Sakata, K., and Mizutani, M. (2004) *Plant Physiol.* **134,** 1439–1449
56. Kushiro, T., Okamoto, M., Nakabayashi, K., Yamagishi, K., Kitamura, S., Asami, T., Hirai, N., Koshiba, T., Kamiya, Y., and Nambara, E. (2004) *EMBO J.* **23,** 1647–1656
57. Buehner, M., Ford, G. C., Moras, D., Olsen, K. W., and Rossmann, M. G. (1974) *J. Mol. Biol.* **82,** 563–585
58. Raisig, A., Bartley, G., Scolnik, P., and Sandmann, G. (1996) *J. Biochem.* (*Tokyo*) **119,** 559–564
59. Al-Babili, S., von Lintig, J., Haubruck, H., and Beyer, P. (1996) *Plant J.* **9,** 601–612
60. Schneider, C., Boger, P., and Sandmann, G. (1997) *Protein Expression Purif.* **10,** 175–179
61. Shirley, M. A., Bennani, Y. L., Boehm, M. F., Breau, A. P., Pathirana, C., and Ulm, E. H. (1996) *Drug Metab. Dispos.* **24,** 293–302
62. Schmidt, C. K., Volland, J., Hamscher, G., and Nau, H. (2002) *Biochim. Biophys. Acta* **1583,** 237–251
63. Derguini, F., Nakanishi, K., Hammerling, U., Chua, R., Eppinger, T., Levi, E., and Buck, J. (1995) *J. Biol. Chem.* **270,** 18875–18880
64. Henikoff, S., and Henikoff, J. G. (1992) *Proc. Natl. Acad. Sci. U. S. A.* **89,** 10915–10919
65. Saitou, N., and Nei, M. (1987) *Mol. Biol. Evol.* **4,** 406–425